Experimental Studies of Breakdown Characteristics of SF_6/CF_4 Mixtures in Highly Non-uniform Fields for High-voltage Applications

By:

Kamran Toufani

April, 1997

Presented to:

The University of Manitoba

In fulfillment of the requirements for the degree of

Master of Science in Electrical Engineering

Winnipeg, Manitoba

Canada

THE UNIVERSITY OF MANITOBA

FACULTY OF GRADUATE STUDIES

*****

COPYRIGHT PERMISSION PAGE

EXPERIMENTAL STUDIES OF BREAKDOWN CHARACTERISTICS OF SF_6/CF_4 MIXTURES IN HIGHLY NON-UNIFORM FIELDS FOR HIGH-VOLTAGE APPLICATIONS

BY

KAMRAN TOUFANI

A Thesis/Practicum submitted to the Faculty of Graduate Studies of The University of Manitoba in partial fulfillment of the requirements of the degree of

MASTER OF SCIENCE

Acknowledgment

I wish to express my deepest gratitude to my advisor Dr. Edmund Kuffel for his invaluable guidance and support during the course of this work. I also wish to extend my special thanks to Dr. Waldemar Ziomek for his help and guidance during the experimental phase of this research. Special thanks is also extended to Dr. M.R. Raghuveer whose expert opinion on high-voltage engineering related problems was of invaluable assistance. I also wish to thank Mr. John Kendall and Mr. Gordon Toole for their help in constructing the apparatus and providing the technical assistance.

The financial supports from Manitoba Hydro and the Natural Science and Engineering Research Council of Canada which made this investigation possible are greatly appreciated.

Abstract

Pure SF_6 liquefies at approximately -33°C at increased pressure range of the practical high-voltage gas-insulated switchgears (3.0-5.0 bar). The use of SF_6/CF_4 mixtures with lower condensation temperature and comparable dielectric properties, is proposed to overcome the SF_6 limitations for operation in extreme cold climates (i.e. Canada). Recent studies have shown that the SF_6/CF_4 mixture when mixed in certain proportions exhibits strong positive synergism for application of ac and dc voltages in highly divergent fields. The present thesis aimed to investigate thoroughly the dielectric strength of SF_6/CF_4 mixtures over the range of pressure used in practical high-voltage apparatus using highly divergent fields and a wide range of mixture compositions. The SF_6/CF_4 mixtures were studied under ac, dc and standard lightning impulse voltages (positive and negative polarities). The time lags for lightning impulse breakdown voltages and corona inception for ac and dc voltages were recorded. The occurrence of strong positive synergism was validated for dc and ac voltage applications in non-uniform fields.

Table of content

List of illustrations

List of tables

I. Introduction

The excellent dielectric properties of SF_6 (sulfur hexafluoride) have lead to its wide range of application in the field of high voltage insulation. In recent years, binary gas mixtures with SF_6 as the main constituent, have been the subject of active research. The objectives were to develop new practical mixtures with the desired properties of SF_6 and to correct the undesired properties to a negligible level. This way, the new combination of gases can be tailored to specific applications.

Recent studies of SF_6 and CF_4 (carbon tetrafluoride) which were designed to develop mixtures for insulation in extremely cold regions (i.e. Canada), have shown that the mixture of SF_6/CF_4 when mixed in certain proportions exhibits positive synergism especially in highly divergent field [14]. The aim of the present thesis was to conclude detailed studies of the dielectric strength of these mixtures over the range of pressure used in practical applications using highly divergent fields and a wide range of mixture compositions.

For completeness the properties of SF_6 will be briefly reviewed, followed by a comparison of the dielectric properties of mixtures comprising more commonly used buffer gases such as N_2 with that of SF_6/CF_4 properties.

I.a. Sulfur hexafluoride

I.a.1 History

In the field of the high voltage insulation, sulfur hexafluoride or SF_6 is known to be an excellent insulating gas; SF_6 owing to its high dielectric strength, chemical

inertness, and good heat transfer properties has been widely used as an insulation medium in gas insulated equipment for several decades. In the past, because of its desired dielectric properties for application in electrical apparatus; SF_6 has been subjected to detailed engineering investigations.

SF_6 was first discovered in 1900, but little scientific interest for practical applications was shown until 1940 when Cooper suggested SF_6 might have a beneficial use as a dielectric gas in high voltage equipment [1,2]. The earlier application was in Van de Graaff generators which caused a growing interest for use in other gas insulated high voltage equipment. At present, SF_6 is extensively used in wide variety of electrical power equipment such as; Gas Insulated Switchgear (GIS), dry transformers and cable technology.

I.a.2. General Properties

SF_6 possesses many advantages as a dielectric gas. It is nontoxic and nonflammable and has a superior cooling characteristic. It has a dielectric strength substantially higher than traditional dielectric gases. In addition, it possesses exceptional arc quenching properties and its use in electrical equipment eliminates fire hazards, allows considerable reduction in size and improves the reliability of the system. At the same time, SF_6 possesses some disadvantages. One major problem is its decomposition under electrical discharges forming lower fluorides of sulfur. These decomposition products are toxic and corrosive to many insulating and conducting materials. Also, the liquefaction temperature under high pressure is relatively low (-33°C at 3.5 bar) and

presents a problem in its application in outdoor high voltage equipment design for extremely cold regions [3]

The physical properties of SF_6 gas are listed in Table 1.1 [4]. SF_6 is a dense gas, the density being 6.164 grams per litre at 20°C and 760 torr. This is approximately 5 times the density of air under similar conditions.

Table 1.1: The physical properties of SF_6 [4]

Molecular Weight	146.06
Melting Point (°C)	-50.8
Sublimation Temperature (°C)	-63.8
Density (solid) at 50°C	2.51 g/ml
Density (liquid) at 50°C and 25°C	1.98 and 1.329 g/ml
Density (gas at one bar and 20°C)	6.164 g/l
Critical Temperature (°C)	45.6
Critical Pressure (bar)	36.557
Critical Density	0.755 g/ml
Specific Heat (25°C - cp)	7.0 g cal/ml°C
Specific Heat (30°C)	0.143 cal/g
Surface Tension (-50°C)	11.63 dyn/cm
Coefficient of Expansion (-18.5°C)	0.027
Thermal Conductivity ($x10^4$)	3.36 cal/sec/cm^2/°C/cm
Viscosity (gas at 25°C $x10^4$)	1.61 poise
Boiling Point (°C)	-63
Relative Density (air=1)	5.10
Expansion on Melting	30%
Vapour Pressure (20°C)	10.62 bar
Refractive Index (N at 0°C)	1.000783
Density (20°C, 1 bar)	6.5 kg/m^3

Chemically, sulfur hexafluoride is a stable gas. At atmospheric pressure, SF_6 possesses a high degree of chemical stability at temperatures up to at least 500°C; at higher temperatures increasing degree of chemical instability is manifested. At temperatures above 500°C, SF_6 will react rapidly with the silicate glasses and with certain metals; but is found to be inert to metals such as copper, steel, and aluminum within the usual temperature range of operation for electrical equipment. Tests have indicated negligible corrosion for various metals when exposed to SF_6 at 223°C for 270 days [5].

SF_6 is non-ignitable and non-flammable. The gas is self-healing after electrical breakdown and no conducting decomposition products such as amorphous carbon are deposited as a result of continuous arcing.

The properties of other fluorides of sulfur are listed in Table 1.2 [4]. These may be present as byproducts of decomposition and contaminants of the SF_6 gas.

Table 1.2: The physical properties of fluoride of sulfur [4]

Property	S_2F_2	SF_4	S_2F_{10}
Odour	sulfurous	odourless	odourless
Melting point (°C)	-105.5	-124	-92
Boiling point (°C)	-99	-40	29
Specific gravity	1.5(-100°C)	-	2.08(0°C)
Toxicity	paralyzes	toxic	poisonous
Reaction with H_2O	decomposes	decomposes	-

SF_6 is a non-toxic gas. Its toxic properties are mainly associated with the presence of the lower fluorides such as SF_2, S_2F_2, S_2F_{10}, SF_8 and HF. These may be present as

impurities because of improper manufacturing or as decomposition products formed under an electric arc. The physiological effects of these decomposition products are not clear. Each has been described as toxic, even though, some of them are only mildly toxic. Since, there is always possibility of the presence of decomposition products either by excessive heat or the electric arc, one must always consider the possibility of gas decomposition products for engineering applications.

I.a.3. Electrical Properties

The high dielectric strength of SF_6 is due to the strong electron attachment properties of the SF_6 molecule. In this process, free electrons collide with the neutral gas molecules to form negative ions by the following process.

$$\begin{aligned} SF_6 + e &\longrightarrow SF_6^- \\ SF_6 + e &\longrightarrow SF_5^- + F \end{aligned} \qquad (1.1)$$

The first equation represents attachment process starting at electron energies of 0.1 eV with an energy range of 0.05 eV. The process shown by the second equation attains a maximum at 0.1 eV. The negative ions formed are heavy compared to the free electrons and therefore under a given electric field the ions do not accumulate sufficient energy to lead to ionization in the gas. This process represents an effective way of removing electrons which otherwise would have contributed to the cumulative ionization, to the current growth and finally to the breakdown of the gas. This property

gives rise to very high dielectric strength for SF_6 gas. Even corona onset voltage for SF_6 in a non-uniform electric field is considerably higher when compared to air.

Numerous measurements of the ionization (α/p) and attachment (η/p) coefficients have been recorded in literature. But these measurements mainly deal with low values of gas pressure. An extrapolation of the values of these coefficients to higher pressures is therefore necessary for most practical applications. The values of $(\alpha-\eta)/p$ as a function of E/p are shown in Fig. 1.1 [6].

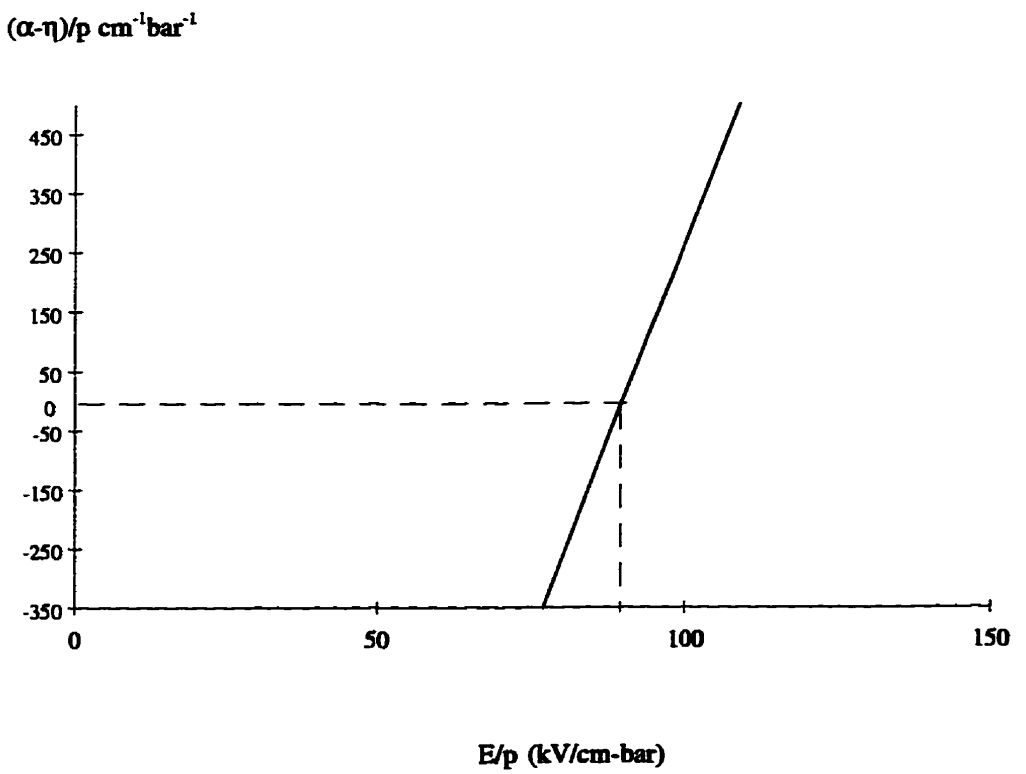

Figure 1.1 $(\alpha-\eta)/p$ vs. E/p characteristics in SF_6 [6]

Over a wide range of gas pressures for uniform field configuration in SF_6, the following empirical equation is found to be valid.

$$\frac{\alpha-\eta}{p} = k[E/p-(E/p)_{limit}] \qquad (1.2)$$

Where E=applied electric field, kV/cm

k= 27.7 kV^{-1}

p=gas pressure in bar, referred to a temperature of 20°C

$(E/p)_{limit}$: limiting value of E/p below which no breakdown is possible ($\alpha=\eta$),

is equal to 88.5 kV/bar.cm or 118 V/torr.cm

The number of free electrons in an avalanche will increase in any region where E/p exceeds $(E/p)_{limit}$ and will decrease when E/p is less than $(E/p)_{limit}$.

Conversely, the non-uniform field is difficult to analyze, but is of considerable importance from the practical point of view since it is the condition most commonly encountered in electrical apparatus. In non-uniform field gaps, all evidence suggests that a strongly field dependent electron production must be present. It is expected that the breakdown caused is by streamer injection, initiated by particles. For highly non-uniform fields, the streamers develop into a steady discharge giving rise to a "corona stabilized" higher breakdown. Generally, it is a common practice to design the apparatus to operate without corona. Therefore with SF_6 gas, the field non-uniformity must be avoided as far as possible. Also, the corona onset voltage should be taken as a criterion for the design where non-uniformity of the field can not be avoided.

Nita [7], in his classical paper, has treated the non-uniform field breakdown in SF_6 both theoretically and experimentally. The equation for the total number of electrons in the avalanche N, for both uniform and non-uniform gaps is given by,

$$\ln N = \int_0^{x_c} (\alpha - \eta) dx \qquad (1.3)$$

x = distance from the electrode which gives the maximum field strength (E_{max}),

x_c = the value of x where $\alpha=\eta$.

Nita used Raether's criterion [8] for transition from avalanche to streamer that is, $N_c \cong 10^8$. For uniform field gaps, E is constant across the gap in Equation 1.3.

$$\ln N = k[E - \{E/p\}_{limit} p]d \qquad (1.4a)$$

with $N = N_c$

$$\frac{E_b}{p} = \frac{\ln N_c}{kpd} + \{E/p\}_{limit} \qquad (1.4b)$$

$$V_b = \frac{\ln N_c}{k} + \{E/p\}_{limit} pd \qquad (1.4c)$$

For non-uniform field, Equation 1.4a becomes

$$\ln N = k[\int_0^{x_c} E(x)dx - (\{E/p\}_{limit} px_c)] \qquad (1.5)$$

Because k is very large in SF_6, x_c is very small to give conditions for streamer. Hence breakdown in non-uniform field in SF_6 is dictated by the electric field distribution near electrodes. Takuma, et al.[9], suggested that the discharge characteristics in high

pressure SF_6 resembles those observed in lightning discharge [9]. In high pressure SF_6, once a leader originates, it is propagated by its own space charge field, even if the field is so weak that $\alpha<\eta$. The local field at the tip is supported by the high conductivity channel. Because of the rapid increase of $\bar{\alpha}$ with E, the breakdown strength in SF_6 is dictated largely by E_{max} in the gap.

SF_6 not only possesses a high dielectric strength, but also, its molecules when dissociated due to sparkovers, recombine rapidly after the source energizing the spark is removed and the gas recovers its strength. This makes SF_6 uniquely effective in the quenching of arcs. It is approximately 100 times as effective as air in quenching arcs. This property of SF_6 is attributed to several factors. SF_6 gas has a large electron attachment coefficient. If the free electrons in an electric field can be absorbed before they attain sufficient energy to generate additional electrons by collisions, the breakdown mechanism can be delayed or even be stopped. The large collision diameter of the SF_6 molecule, estimated to be 4.77 Å, assists in capturing these electrons by attachment processes thus giving rise to stable negative ions. Energy is also stored in the vibrational and rotational levels of the SF_6 molecules. The negative ions so formed reduce the effect of the positive ion space charge around the electrodes, cathode particularly, and thus necessitate the application of a higher voltage to produce an arc across the gap. The high heat transfer capability and the low arc temperature provide SF_6 with an excellent capacity for extinguishing electric arcs [4,10]. The heat transfer properties essentially consist of the specific heat of the gas, thermal

conductivity and the viscosity. In general, SF_6 has good heat transfer characteristics; from the general characteristics of SF_6 gas upon establishment of a thermal gradient in the gas, its lower viscosity coupled with its greater density would lead to more extensive gas circulation than would be obtained in nitrogen or air under the same thermal conditions in commercial gas filled equipment. This should result in better heat dissipation from the operating parts of such equipment. The final result would be a cooler temperate of operation in SF_6 gas filled equipment and this has been experimentally found to be true [11].

I.b. Binary gas mixtures with SF_6

Utility companies desire to have a system which once installed can be left alone with the assurance that it will perform worry-free for the next 35 years. In addition, the system has to be simple to install and maintain, besides its economic feasibility. Therefore, it must utilize the insulating materials that possess excellent dielectric properties. Regarding gas insulators with today's stringent environmental constraints, the insulating gas medium must be environmentally acceptable not only in its original state but also after sustaining an arc caused during a fault. The insulating gas must remain in gaseous state throughout the operating temperature cycle and operating pressure. The cost of gas contributing to the cost of overall system must lie within the tolerance margins of economical feasibility [12]. Since no single gas meets all the requirements imposed by recent demands on power systems, gas mixtures seems to be

an appropriate alternative. Using a gas mixtures as the insulating medium, the properties of component gases can be exploited to suit the demands for specific application. A cheaper gas can be substituted for part of SF_6 while maintaining the desired dielectric strength or the overall cost of system can be reduced using a component gas which can operate in a smaller enclosure due to its higher than SF_6 dielectric strength. Alternatively, improvement of system reliability can be achieved using a component gas whose breakdown strength is less sensitive to particle contamination and surface roughness.

Sulfur hexafluoride (SF_6) because of its excellent dielectric properties discussed earlier, is chosen to form the base gas in the binary or even tertiary mixtures. Gas mixtures with SF_6 as the base gas for insulation applications have been proposed; such mixtures, although with reduced dielectric strength tend to be less sensitive to particle contamination or surface roughness [13].

To choose a mixture for practical insulation application, investigation normally focuses on the breakdown sensitivity to particle contamination and surface effects, synergism, arc quenching, reliability, economical consideration and etc.

I.b.1. Mixture of Sulfur hexafluoride and Nitrogen

Nitrogen (N_2) is one of the appropriate candidates to be mixed with SF_6. Nitrogen is a buffer gas and has no electronegative properties. Due to the low condensation temperature of nitrogen, it is especially suitable for use in the regions of extreme cold

(i.e. Canada). Addition of a buffer gas to SF_6 slows down high energy electrons and brings them into an energy range where they may be captured via electron attachment by SF_6. Nitrogen is relatively inert and can be provided inexpensively due to its abundance [14]. When the breakdown strength of a mixture is higher than the sum of corresponding breakdown strength of the constituent gases weighted by their partial pressure at the same pressure, it is said that the components act in a cooperative or synergistic manner to increase the dielectric strength of the mixture. As practical insulants, strongly attaching gases suffer from the disadvantages of high cost and low liquefaction pressure; however if small quantity of electronegative gas is added to a gas such as nitrogen, a very large increase in its dielectric strength will be acquired [3]. The previous findings indicate some promising performance of SF_6 and nitrogen mixture. For example, a 50%/50% SF_6 and nitrogen mixture exhibits the same dielectric strength as 85% SF_6 but at approximately 35% lower cost when operating at 15% higher pressure [13]. As mentioned earlier, the local field enhancements caused by surface roughness or sharp edges lower the SF_6 breakdown strength. The mixtures of SF_6/N_2 have been found to be less susceptible to particle contamination breakdown than pure SF_6 [15,16]. These mixtures provide a viable alternative to pure SF_6 without the necessity to raise greatly the total pressure of a system.

As mentioned earlier, a certain advantage of SF_6/N_2 mixture over pure SF_6 is its capability in controlling particle contamination. In SF_6-insulated equipment, the dielectric strength is often lowered drastically by unavoidable contaminating particles.

Table 1.3 presents breakdown voltage of SF_6/N_2 mixtures in coaxial cylinder electrode geometry and contamination simulated by copper test particles [17]. The electrical stress is imposed by dc voltages. This set of breakdown measurements in SF_6/N_2 mixtures of different proportions and pressures, suggests an optimum proportion of SF_6 and N_2 (60%-SF_6/40%-N_2) and also there exists an optimum total pressure which may vary somewhat with conditions.

The application of gas mixtures for transformers and circuit breakers is in its early stage when compared with transmission lines. Again, the benchmark gas is SF_6 to which we compare the performance of other gas mixtures. Circuit breakers in addition to dielectric strength, require the arc quenching capability of their insulating gas to

Table 1.3: Breakdown voltages of SF_6/N_2 mixtures in particle-contaminated concentric cylinder geometry under dc Stress

Percentage		Breakdown Voltage (kV)				
SF_6	N_2	300kPa	400kPa	600kPa	800kPa	1000kPa
100	0	59.6	62.1	70.0	67.5	60.0
80	20	45.7	49.0	59.6	58.6	50.1
60	40	50.7	54.1	66.0	62.4	61.2
40	60	24.3	39.5	55.7	50.9	43.5
20	80	26.3	38.5	37.2	41.9	33.4

extinguish the arc and to recover its dielectric properties. Also, practical circuit breakers are designed to operate at increased pressure (3.5-5.0 bar); however, pure SF_6 will liquefy at that pressure range at approximately -33°C. The use of appropriate

mixtures with lower condensation temperatures and similar arc quenching properties to SF_6 may overcome the limitation of using SF_6 alone in circuit breakers designed for operation in extreme cold climates. Earlier applications of SF_6/N_2 mixtures in circuit breakers had overcome the problem, but it has been found that increasing the percentage nitrogen causes a drop in interrupting capability of the mixture and the circuit breaker had to be downrated [18].

To overcome the reduction in thermal capability of SF_6/N_2 gas mixtures and to maintain a full interrupting rating of equipment should fault condition arise, one possible option might be to compensate for the reduced thermal capability by including more grading capacitors across the apparatus (circuit breaker or disconnector) as well as shunt capacity connected at the line side. Unfortunately, choosing too high a value of grading capacity poses an increased risk of ferroresonance condition. Furthermore, addition of shunt capacity involves an imposed large expense which in most cases is not economically feasible. A second possible option is to select a gaseous dielectric that maintains the thermal capability of SF_6 while at the same time retaining a low condensation temperature as that of SF_6/N_2 mixture. SF_6/CF_4 mixtures satisfy the very low liquefaction temperature requirement of SF_6/N_2 mixtures and in addition, they possess better arc quenching property which makes them a more appropriate candidate for use in circuit breaker technology.

I.b.2. Mixture of Sulfur hexafluoride and Carbon tetrafluoride

Gaseous fluorocarbons including CF_4, have long been of interest in high voltage applications due to their inert character and high dielectric strength. Fluorine is a rather unique element, It is the most reactive element in the periodic table and reacts with nearly all other substances with the interesting result that many of the combinations are among the most inert substances. A very familiar example is SF_6 which is chemically, thermally and electrically very stable. Other fluorogases including Freons and fluorocarbons offer high dielectric strength, low liquefaction temperature, chemical inertness, non-toxicity, non-flammability and good heat conduction. Flurocarbon gases manifest wide variations in dielectric strength, however all invariably show a breakdown voltage which is greater than that of air or nitrogen. Figures 1.2 and 1.3 show the dielectric strength of CF_4, SF_6, air and nitrogen with respect to pressure when tested under positive standard lightning impulse and 60 Hz ac voltages [21,22].

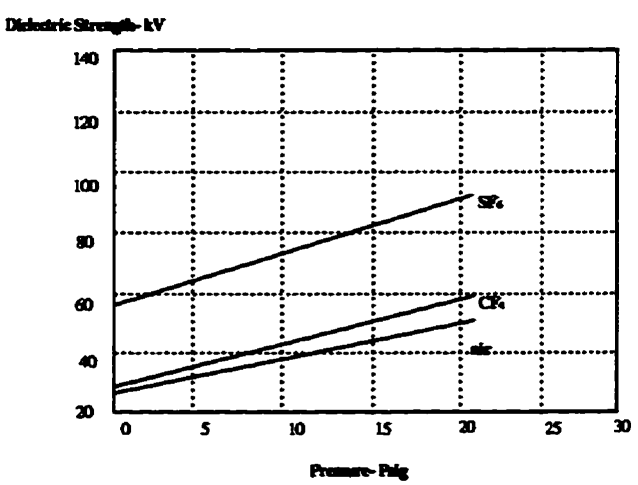

Figure 1.2 Positive standard lightning impulse breakdown (rod-sphere electrode, 25.5 mm gap separation) [21]

In a quasi-uniform field configuration (Fig. 1.2), the dielectric strength of SF_6 remains substantially higher than that of CF_4 for standard lightning impulse tests and for all pressures tested [21]. For the same series of tests, the dielectric strength of CF_4 is comparable to that of air but is slightly higher. For a uniform field configuration and 60 Hz breakdown voltages (Fig. 1.3), the dielectric strength of CF_4 (F14) is almost halfway between the dielectric strengths of SF_6 and N_2; the SF_6 and nitrogen dielectric strengths being the upper and lower limits respectively [22].

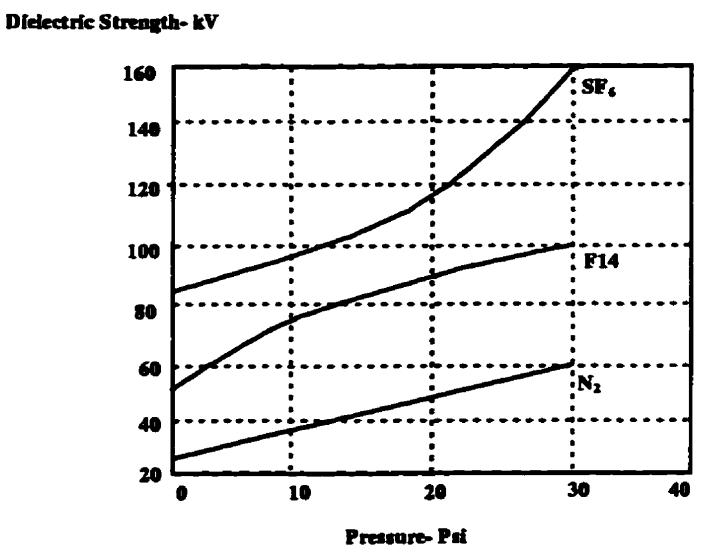

Figure 1.3 60 Hz breakdown voltages (planar electrodes of 76.2 mm^2, 12.75 mm gap Separation) [22]

CF_4 has good electron attachment properties for electron energies higher than 2.5 eV and from Table 1.4, it can be seen that CF_4 has a much lower critical temperature[1]

[1] The temperature above which a gas can not be liquefied by the application of pressure.

and much higher critical pressure[2] than all other fluorocarbons in that table. Both low critical temperature and high critical pressure are very desirable properties for gaseous dielectrics [23,14].

Table 1.4: Properties of selected fluorocarbons [3]

Formula	Rel. dielectric strength	Boiling point (°C)	Freezing point (°C)	Critical temp. (°C)	Critical press. (°C)
CF_4 (F-14)	1.3	-128.0	-184.0	-47.3	3723.2
C_2F_6	1.8	-78.0	-101.0	24.3	3288.8
C_3F_8	2.0	-37.0	-160.0	70.5	2675.2
C_4F_{10}	2.5	-2.5	-80.0	113.0	2013.3
C_5F_{12}	2.8	29.3	-125.5	-	-

The difficulty associated with the use of CF_4 as a dielectric is its generic label, Freon-14. Back in mid-1950's, the Freon gases were considered ideal alternatives to ammonia for refrigerants due to their good chemical stability and low toxicity to humans; CF_4 was defined by government standards as Freon-14. Freons are characterized by a high dielectric strength which in some instances has been cited to be more than 8 times that of nitrogen [23]. It was not known back in mid-50's that the concentration of Freon gases in atmosphere deteriorates ozone layer via chemical reaction. Subsequently, a significant depletion of the atmospheric ozone layer has prompted authorities to impose a global ban on the synthesis of all Freon gases by 1997. Although CF_4 has been labeled Freon-14, this is a misnomer because Freon gases

[2] The minimum pressure under which a substance may exist as a gas in equilibrium with the liquid while being maintained at its critical pressure.

typically contain atoms of carbon, fluorine and chlorine and are referred as chlorinated fluorocarbons (CFC). Chlorine is the element responsible for atmospheric ozone layer depletion through chemical reaction and CF_4 is the only Freon gas that does not contain chlorine, therefore is not harmful to the ozone layer. Unfortunately, it had been a government decision that wrongfully banned the labeled CF_4. Therefore, unless any lobbying can be accomplished to classify CF_4 as a non-Freon, its use as a dielectric gas in SF_6 mixtures is terminated [14].

II. Experimental set up

II.a. Gap Arrangement

In order to simulate the condition of highly non-uniform field, a point and sphere gap arrangement was chosen. The respective dimensions were:

Point: a 10 mm diameter brass rod tapered 30° to a tip which was a spherical cap of radius 0.5 mm,

Sphere: copper, 62.5 mm diameter.

The experiments were carried out with gap separations of 5-30 mm, increased in 5 mm steps.

II.b. The test chamber

The test chamber was a fiberglass reinforced resin cylinder (350 mm diameter, 825 mm height) enclosed by a brass plate (560 mm diameter, 20 mm thickness) at each end as shown in Figures 2.1 and 2.2. The rated pressure of the vessel was specified at 700 kPa by the manufacturer. Due to its age and safety consideration, the experiments were limited to a maximum pressure of 300 kPa. The point and sphere electrodes were supported by an acrylic frame. It consisted of a major structure and a minor structure both positioned inside the chamber (Figure 2.1). The adjustability for the gap arrangement was provided by a dc motor and gear box assembly positioned on the minor frame such as to be able to rotate the bottom earthed electrode (sphere). The shaft of the earthed electrode had a thread pitch such that 341.1° of revolution corresponded to 1mm of vertical displacement.

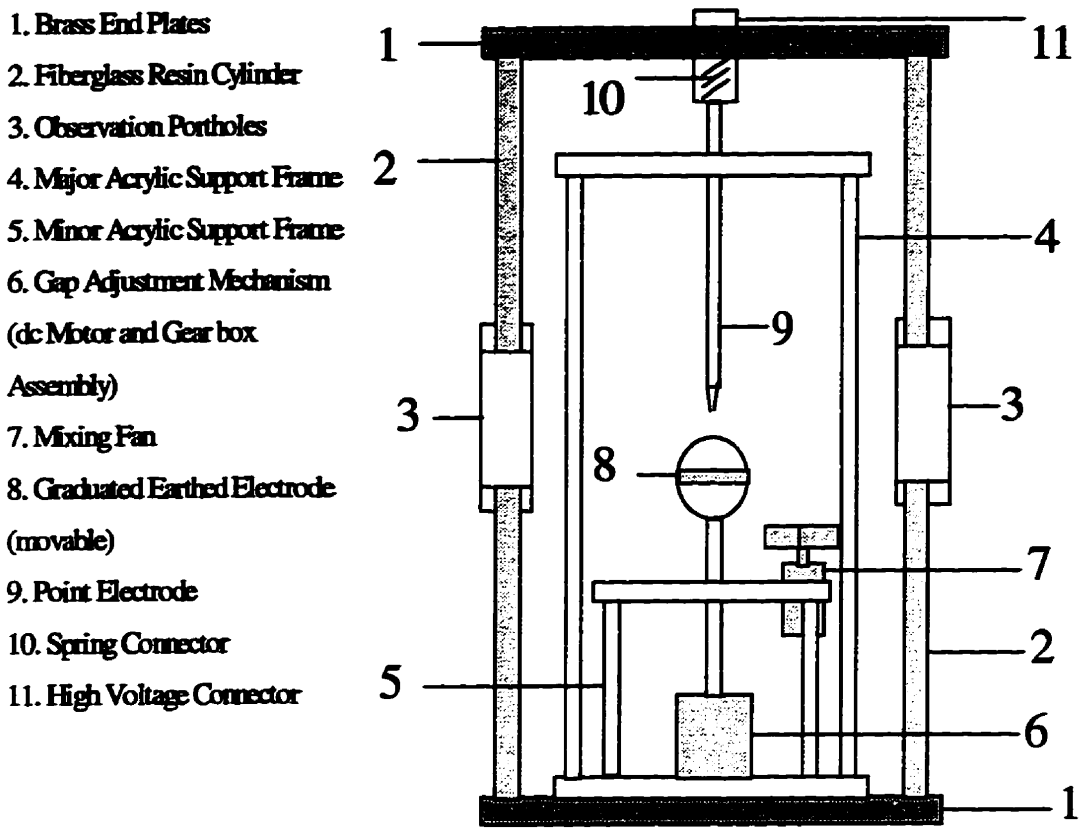

Figure 2.1 Cross section of the test chamber (not to scale)

The equator of the sphere electrode was graduated in degrees in steps of 10° each. The position of each marker with a crosshair on one of the observation portholes provided the precision measurement of revolution. The gaps were adjusted with an accuracy of ±0.015 mm without opening and depressurizing the test chamber each time. The operation and direction of rotation of the gap adjustment mechanism was controlled by two double pole double throw switches from outside the test chamber.

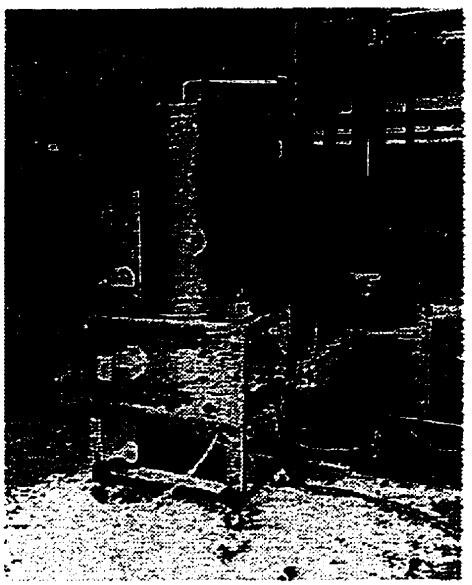

Figure. 2.2 Photograph of the test chamber

II.c. Gas Filling Procedure and Pressure Monitoring

Before sealing the test chamber, all the mechanical and electrical components were inspected thoroughly for proper operation. Some routine refitting work was performed on the pressure valves and o-rings at the interface between the fiberglass cylinder and two brass endplates. Prior to filling the test chamber, the vessel was evacuated to 0.0013 kPa and flushed with prepurified nitrogen (99.995%). The vessel was evacuated a second time to a pressure of 0.0013 kPa. The gas mixtures were admitted into the chamber and the pressure was monitored by a Matheson pressure gauge (±0.25% error, shown in Figure 2.3) against any leakage. The procedure for admitting a particular SF_6/CF_4 gas mixture into the chamber is listed in Appendix A.

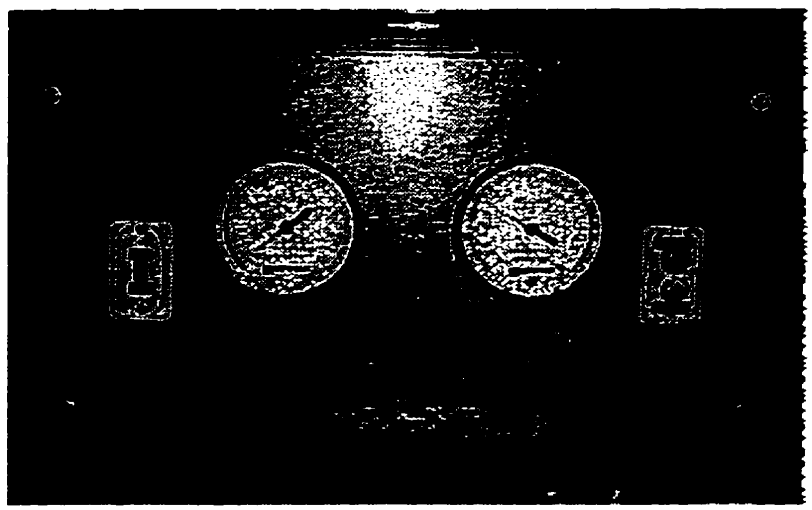

Figure 2.3 The vacuum and pressure monitoring gauges

II.d.. Test Circuits

The experiments were carried out under:

1. Positive and negative standard lightning impulse,
2. Positive and negative polarity dc voltage,
3. 60 Hz ac voltage.

The schematic of the Circuit for generating positive and negative standard lightning impulses (≈1.2×50 μsec) is shown in Figure 2.4. Figure 2.5 shows the photograph of the impulse generator.

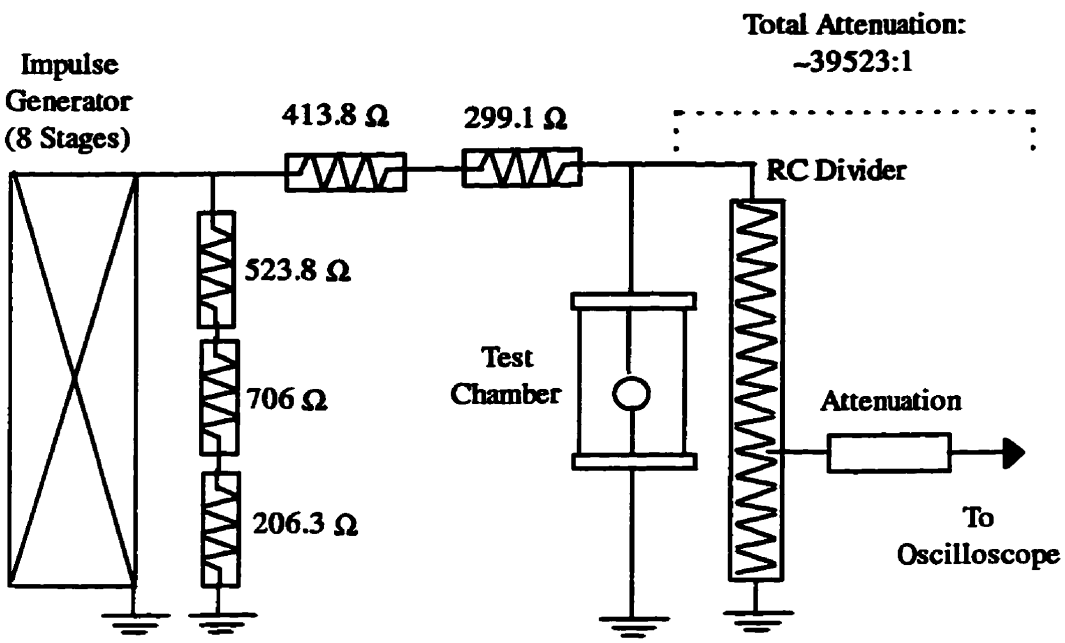

Figure. 2.4 The circuit used for generating standard lightning impulse voltages

The positive and negative standard impulse voltages were generated in accordance with the international standard IEC 60, (IEC 60-2: 1973; Guide on high voltage testing techniques, Part 2. Test procedures) and (IEC 60-4: 1977; Guide on high voltage testing techniques, Part 4. Application guide for measuring devices) [24,25]. The up and down method was used to determine the 50% breakdown voltages of SF_6/CF_4 mixtures. At least, 20 shots were applied for each test on each gap setting for a specific mixture.

Figure. 2.5 Photograph of the impulse voltage generator

The circuit used for application of positive and negative polarity dc voltages to the SF_6/CF_4 gas mixtures is shown in Figure 2.6. Figure 2.7 shows the high voltage dc generator. The control unit of the high voltage dc generator had precision analog voltmeter and ammeter built in and these meters were used to monitor the initiation of breakdowns.

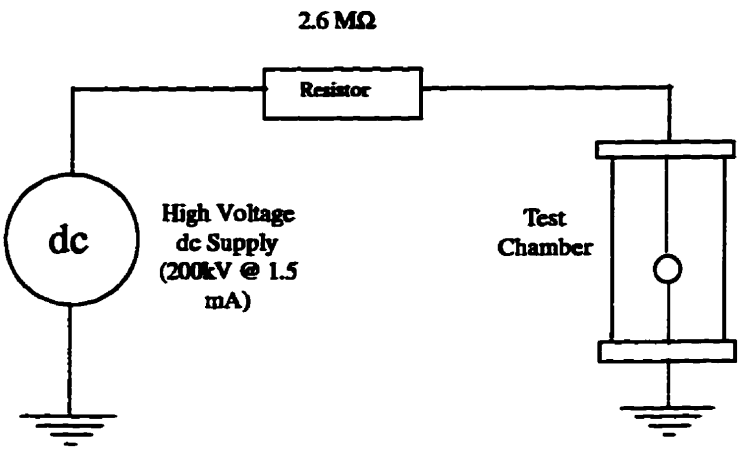

Figure. 2.6 The circuit used for testing of positive and negative polarity dc breakdown

Figure 2.7 High voltage dc generator

The circuit used for application of ac voltage to gas mixtures is shown in Figure 2.8. Figure 2.9 shows the high voltage ac transformer. The precision analog peak voltmeter built in the control panel of the high voltage ac transformer was used for monitoring breakdowns.

For both dc and ac, the inception of corona was determined by connecting a monitoring circuit (Figure 2.10) in series with the ground connection of the test chamber. The output of this circuit was fed to a cathode ray oscilloscope. The circuit depicted in Figure 2.10 consisted of a voltage divider with the dividing ratio of approximately 1/100 and the attenuated voltage was directed to the cathode ray oscilloscope for waveform observation.

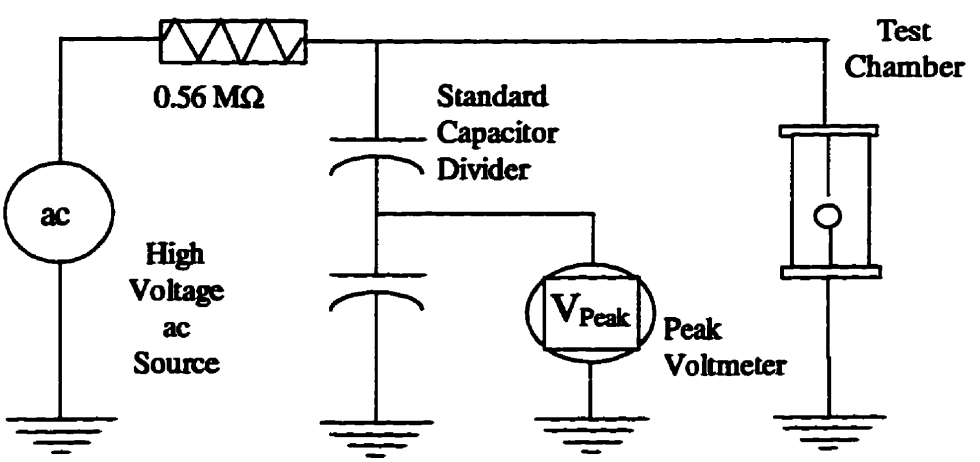

Figure 2.8 The circuit used for testing high voltage ac breakdown

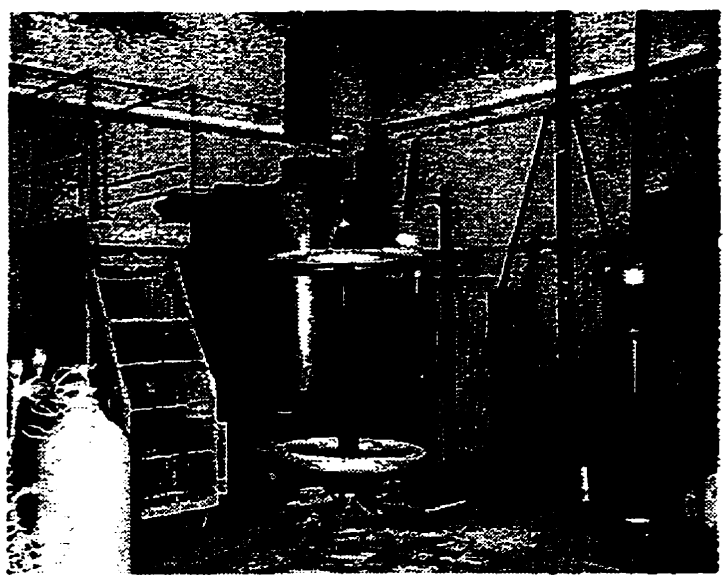

Figure 2.9 The high voltage ac transformer

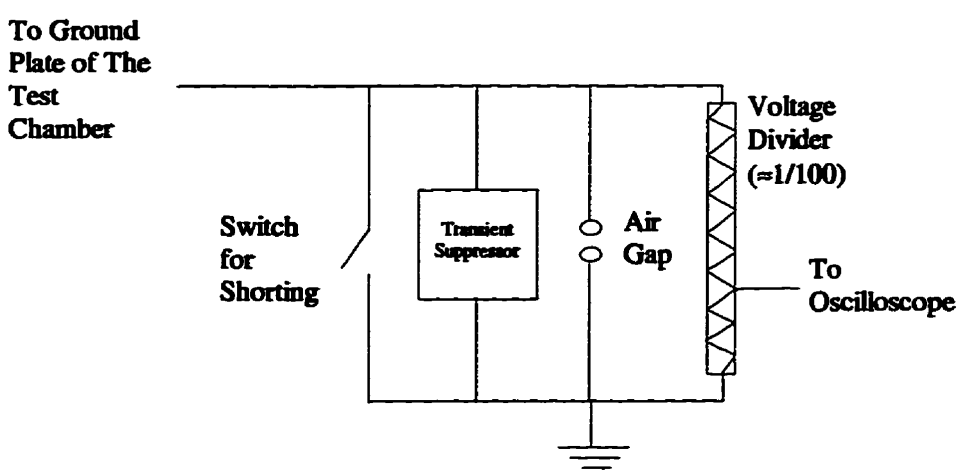

Figure 2.10 Circuit used to monitor corona inception

During testing, the cathode ray oscilloscope was protected against transient overvoltages by means of a semiconductor transient suppresser and an air gap both placed in parallel with the voltage divider. For the breakdown experiments; this circuit was shorted thus making a direct connection between the bottom plate of the test chamber and the ground.

The testing procedure for both dc and ac breakdown and corona inception measurements was conducted according to the guidelines specified in the international standard IEC 60, (IEC 60-2: 1973; Guide on high voltage testing techniques, Part2. Test procedures) and (IEC 60-4: 1977; Guide on high voltage testing techniques, Part4. Application guide for measuring devices) [24,25]. According to IEC 60-2: 1973 guidelines, the dc or ac voltage should be applied to the test object starting at a value sufficiently low to prevent any effect of overvoltage due to switching transient. It should be raised slowly to permit accurate reading of the instruments, but not so slowly as to cause unnecessary prolongation of stressing of the test object near to the test voltage. The above requirements were met by keeping the rate of rise above 75% of the estimated breakdown voltage about 2% per second of this voltage. Not less than 5 voltage applications were made for each test with a 1 minute waiting interval between each application. The voltage had applied and raised accordingly until a disruptive discharge occurred.

The result of the above tests appears as a series of n voltage values U_v from which estimates of the mean disruptive discharge voltage $\bar{U}$ and of the standard deviation s can

be obtained.

$$\overline{U} = \frac{1}{n}\sum_{1}^{n} U_v \tag{2.1a}$$

$$s = \sqrt{\frac{1}{n-1}\sum_{1}^{n}(U_v - \overline{U})^2} \tag{2.1b}$$

The mean breakdown and corona inception voltages for dc and ac series of experiments were determined using Equations 2.1a and 2.1b. The values were corrected for optimal temperature and pressure using the following equation.

$$U_{Corrected} = \left(\frac{Pressure[kPa]}{101.325[kPa]}\right).\left(\frac{295.15[^oK]}{Temperature[^oK]}\right).\overline{U} \tag{2.2}$$

Figure 2.12 shows the view of the high voltage laboratory, University of Manitoba where the experiments were conducted.

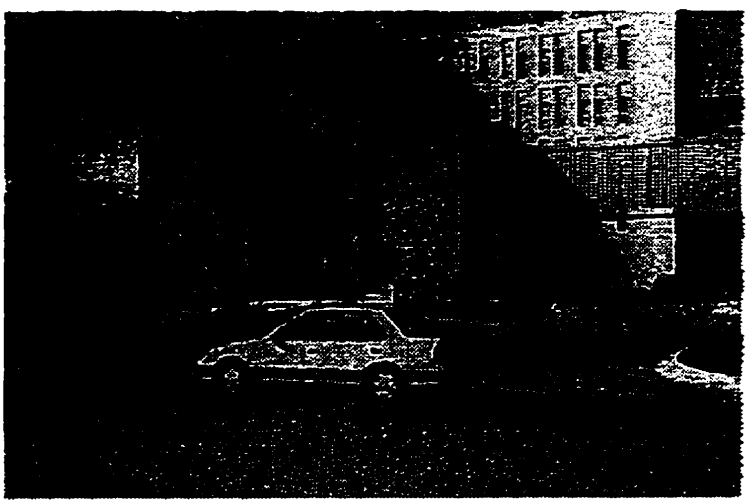

Figure 2.11 High voltage laboratory, The University of Manitoba

III. Experimental Results and Discussion

III.a. Results

The recent study of SF_6/CF_4 gas mixtures breakdown characteristics in highly non-uniform fields by Berg [14] was conducted at a fixed pressure of 200 kPa. The tests were carried out under standard lightning and switching impulse breakdown, positive polarity dc and 60Hz ac voltages. His study covered pure SF_6 and CF_4 and SF_6/CF_4 mixtures with 10, 25, 50 and 75 percent of SF_6 by volume. The gap lengths were 10, 20, 25 and 30 mm (point and sphere electrode arrangement). No SF_6/CF_4 mixture with less than 10% of SF_6 content was investigated.

A strong positive synergism was observed to occur in gaps longer or equal to 20 mm. For standard lightning impulse breakdowns, 100% SF_6 defined the upper limit of breakdown voltage whereas for positive polarity dc the 100% SF_6 breakdown strength was between the mixtures of SF_6/CF_4 and 100% CF_4 (pure CF_4 as the lower limit). A large increase in breakdown strength after adding the first 10% of SF_6 to CF_4 occurred for the positive polarity dc and 60 Hz ac breakdown data. Berg found for all gap lengths that, the standard lightning impulse breakdown voltage increased linearly versus increasing $\%SF_6$ in the mixtures with $\geq$ 10% SF_6 per volume, while the positive polarity dc and 60 Hz ac test results showed a definite positive synergism with the highest breakdown voltage values noted for the $\approx$25%SF_6-75%CF_4 mixtures.

In the present research, however the gas mixtures consisted of 12 different proportions of SF_6 and CF_4 with more emphasis put on mixtures with less than 40% of

the SF_6 content per volume. The gas mixtures ranged from pure CF_4 to 40%SF_6/60%CF_4 with increments of 5% per volume being added to SF_6 content while keeping the pressure constant at 300 kPa absolute. The remaining of mixtures consisted of 65%SF_6/35%CF_4, 85%SF_6/15%CF_4 and pure SF_6 at 300 kPa. The gaps were set to 5, 10, 15, 20, 25 and 30 mm respectively. The pressure of 300 kPa was chosen to represent an approximate pressure encountered in practical compressed gas high-voltage apparatus.

III.a.1 Summary of results on ac(60 Hz) breakdown tests

Figure 3.1 depicts ac (60 Hz) breakdown voltages plotted versus the SF_6 content of the mixture. A highly pronounced positive synergism is observed for 20, 25 and 30 mm gaps in mixtures with SF_6 content ranging from 5 to 35 percent. Notably, there is a sudden decrease in the breakdown voltage for 20 mm gap at the point corresponding to 20% SF_6 content. Also note that the region of positive synergism stays flat for 25mm and 30mm gaps (0-30% SF_6).

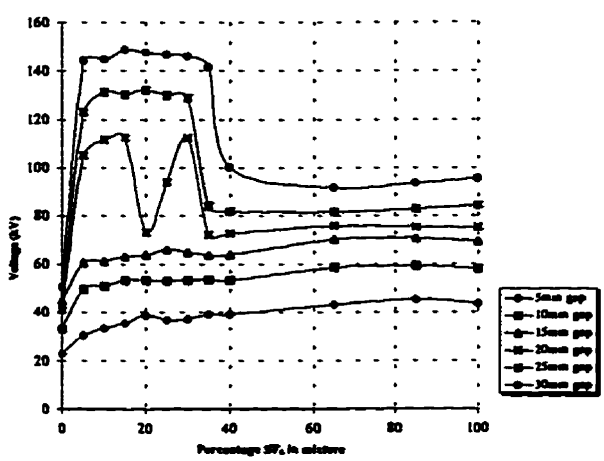

Figure 3.1 Average ac breakdown voltage (60 Hz) as a function of SF_6 content in mixture, 300 kPa

As it was clearly noted in Figure 3.1, a strong positive synergism exists for the mixtures with SF_6 content 5-35% per volume and 20-30mm gap settings. Figures 3.2-3.4 present the ac (60Hz) results plotted against gap separation.

In Figure 3.2, a rapid increase more than 50 kV in average breakdown voltage is evident for mixtures with 5-15% SF_6 and gaps larger than 15 mm. The respective curves closely follow a common trend differing slightly in their average breakdown voltages. For the curve of 20%SF_6/80%CF_4 mixture, the same trend is noticeable but the sudden jump in breakdown voltage has shifted toward the 20mm gap. Figure 3.3 shows the average ac breakdown voltages for the mixtures with SF_6 content 20-40% per volume. The same trend marked by sudden jumps of breakdown strength is evident; but this time, shifting back to 15 mm gap for 25%SF_6/75%CF_4 and 30%SF_6/70%CF_4 mixtures and then shifting forward to 25 mm gap for the 35%SF_6/65%CF_4 mixture. Finally, the positive synergism starts to disappear for the 40%SF_6/60%CF_4 mixture.

In Figure 3.4, the results presented for mixtures with 65 and 85 percent of SF_6 content and the pure SF_6 show slightly higher ac breakdown than the 40%SF_6/60%CF_4 mixture for gaps smaller than 25 mm; for 30 mm gap, their breakdown strength falls below that of 40%SF_6/60%CF_4 mixture. Figure 3.5 shows the average ac breakdown and corona inception voltages plotted versus SF_6 content for the 30 mm gap. Except for the 40%SF_6/60%CF_4 mixture (≈45 kV difference between corresponding maximum and minimum points); the scatter of results is small.

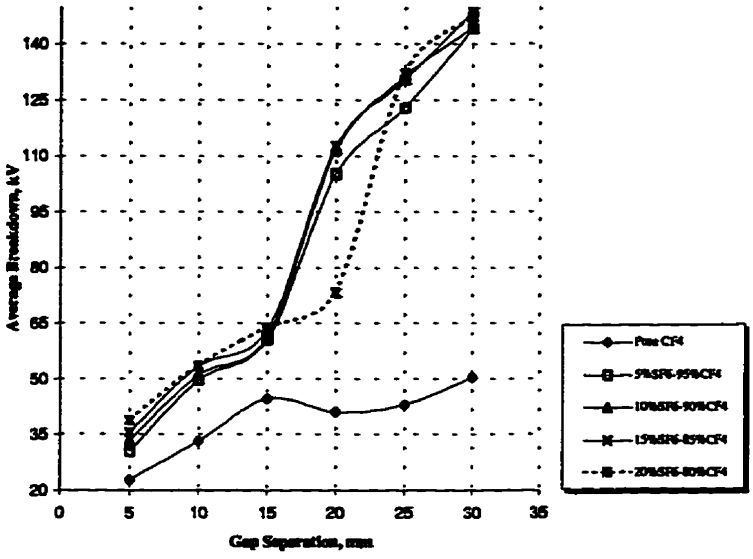

Figure 3.2 Average ac breakdown voltage for mixtures with SF_6 content 0-20% versus gap length, 300 kPa

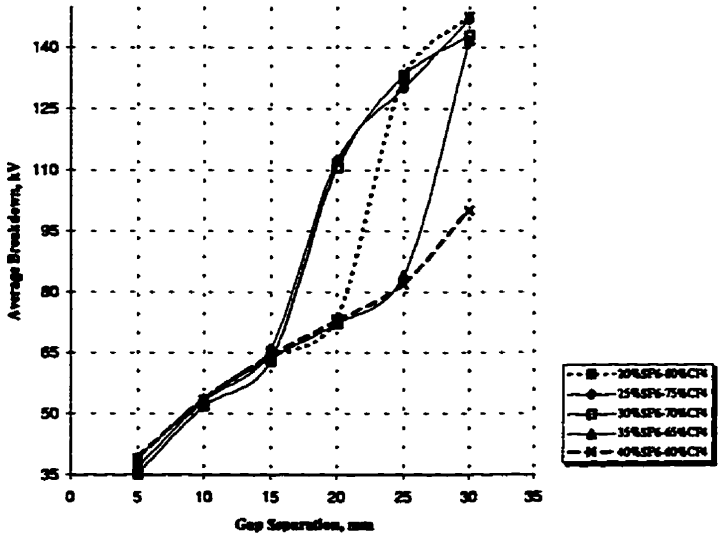

Figure 3.3 Average ac breakdown voltage for mixtures with SF_6 content 20-40% versus gap length, 300 kPa

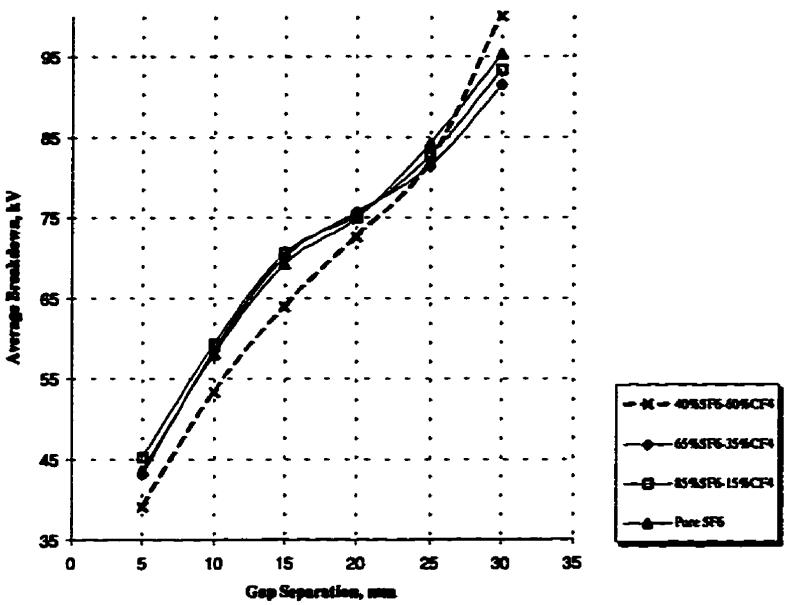

Figure 3.4 Average ac breakdown voltages for mixtures with SF_6 content 40-100% versus gap length, 300 kPa

This displays a high level of certainty for most of the ac breakdown points. The corona inception voltages start at a low level for 5%SF_6/95%CF_4 mixture and increase linearly until the region of positive synergism ends. At this point, the breakdown voltage falls abruptly; suggesting a strong corona stabilization effect.

The same trend applies to 25mm gap (Figure 3.6) with some minor differences such as, smaller scatter for the mixture with 40% SF_6 content.

For the 20 mm gap (Figure 3.7), a double lump in the breakdown voltage is observed. Similar trends for corona inception voltages are observed for 20, 25 and 30 mm gaps.

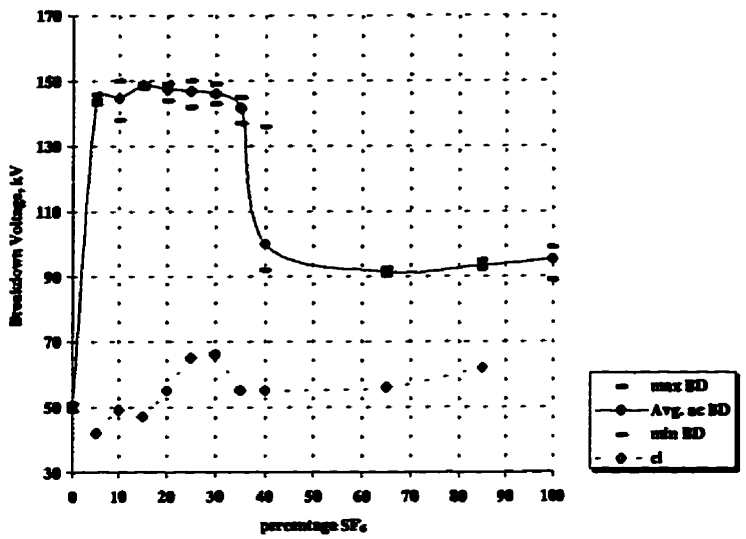

Figure 3.5 Average ac breakdown voltage for 30 mm gap as a function of the SF_6 content, 300 kPa

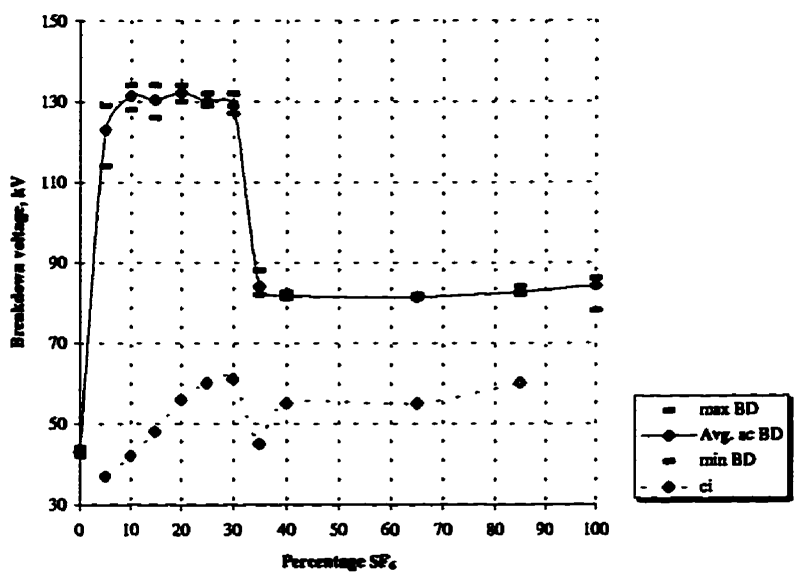

Figure 3.6 Average ac breakdown voltage for 25 mm gap as a function of the SF_6 content, 300 kPa

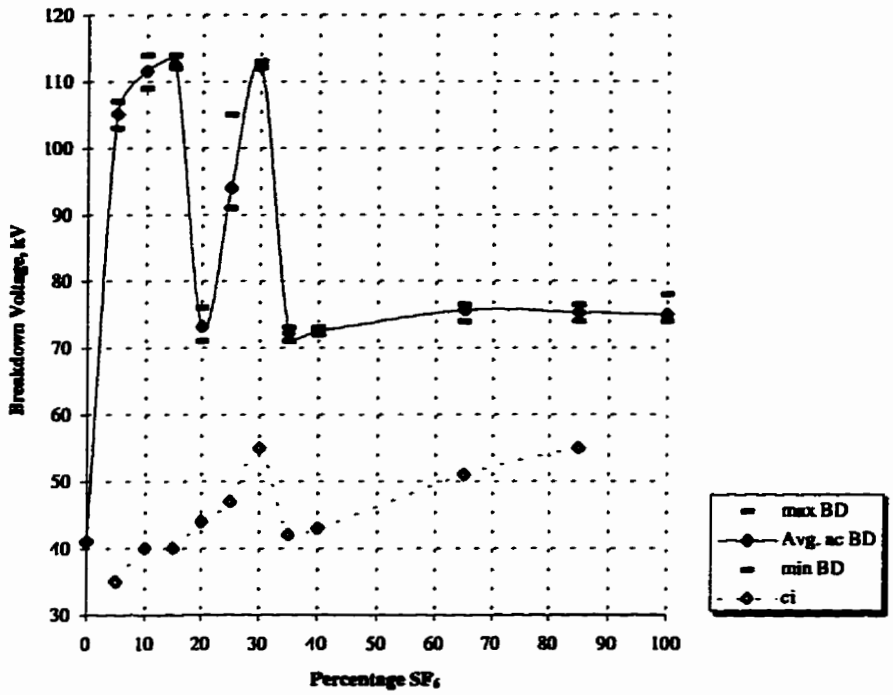

Figure 3.7 Average ac breakdown voltage for 20 mm gap as a function of the SF_6 content, 300 kPa

III.a.2 Summary of results on dc breakdown tests

Figure 3.8 shows the positive polarity dc breakdown voltages versus the %SF_6 content in the mixture. The positive synergism is noted early this time at 10 mm gap. For 10-20mm gaps, synergism extends to 40 percent SF_6 content decreasing slightly at 35% SF_6. However, for 25 mm and 30 mm gaps, the synergism starts falling in two stages; first at 15% SF_6 and next at 30% SF_6 content. For 25 mm gap and 40% SF_6 content; the value of breakdown voltage drops below the breakdown voltage for 20 mm gap.

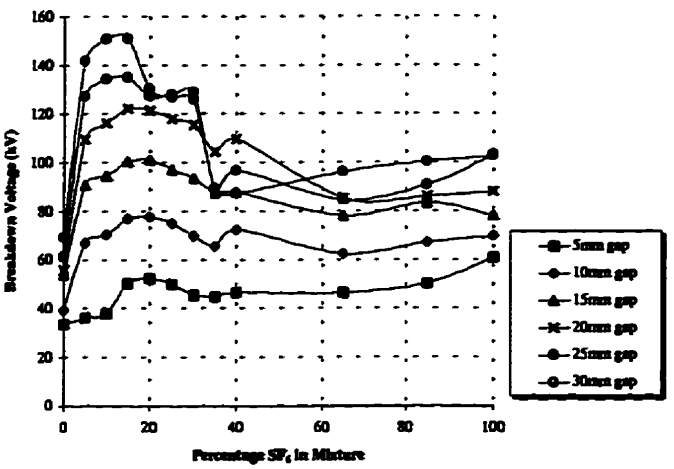

Figure 3.8 Average positive polarity dc breakdown as a function of SF_6 content in mixture, 300 kPa

Under positive polarity dc, a strong positive synergism is observed for mixtures with 5-35% SF_6 content. This positive synergism is more pronounced for 25-30mm gaps. Figures 3.9-3.11 show the average positive polarity dc breakdown voltage plotted against the gap separation. In Figure 3.9, the breakdown voltage increases linearly with spacing for the mixture with 5% and 10% SF_6 content. The breakdown voltage starts to fall at 20 mm gap for 15% SF_6 content. For 20% SF_6 content, the breakdown voltage for 30 mm gap is lower than those of other mixtures with the exception of pure CF_4. In Figure 3.10, the 20 mm gap marks the drop in breakdown voltage again; noting mixtures with 35% and 40% SF_6 for gaps larger than 20mm. The 40%SF_6/60%CF_4 mixture behaves erratically for 5-15 mm gaps; the breakdown strength of this mixture is fluctuating among other mixtures.

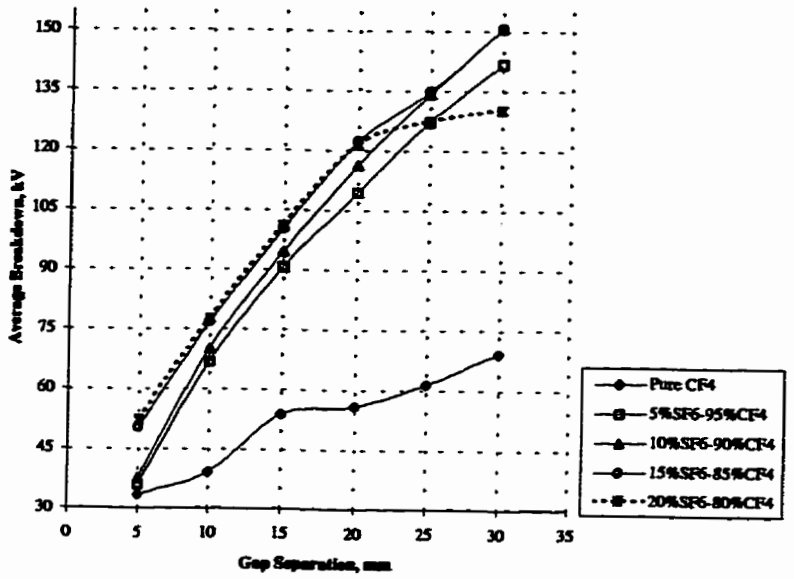

Figure 3.9 Average positive polarity dc breakdown versus gap separation, 300 kPa

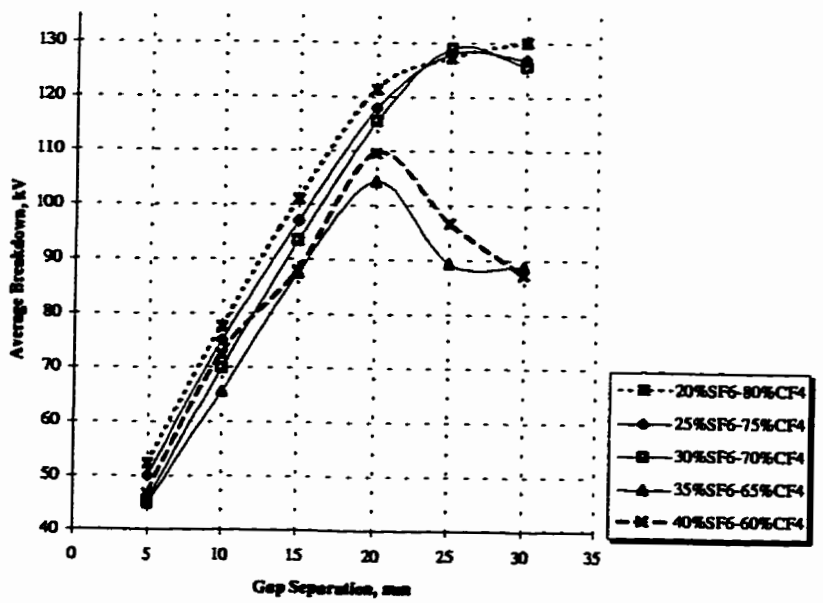

Figure 3.10 Average positive polarity dc breakdown versus gap separation, 300 kPa

Figure 3.11 shows the positive polarity dc breakdown voltage for mixtures with SF_6 content equal and more than 40%. The mixtures behave erratically and the corresponding curves cross each other; the sharp decrease in positive polarity dc strength of the 40% SF_6 mixture for gaps larger than 20 mm is not observed for other mixtures. The increase of dc breakdown strength for pure SF_6 is linear up to 25 mm gap; furthermore, two curves representing 65%SF_6/35%CF_4 and 85%SF_6/15%CF_4 follow each other closely.

Figure 3.12 depicts the average negative dc breakdown strength for mixtures with 5-25% SF_6 content. The result shows high breakdown voltages and a sharp linear increase in breakdown voltage with increasing gap length; similar to positive polarity (Fig. 3.9), for this range of SF_6 content showed a linear increase in breakdown voltage up to 20 mm gap and after that descending breakdown strength for 25%SF_6/75%CF_4 (diminishing positive synergism).

In Figures 3.13-3.18, the average positive and negative dc breakdown and corona inception voltages are plotted versus the percentage of SF_6 in mixture. The certainty of breakdown voltage points is indicated by respective maximum and minimum breakdown voltage points. The corona inception voltage curves follow the breakdown voltage curves such that, a higher breakdown voltage normally corresponds to a lower corona inception voltage. An anomaly is observed for 5 and 10 mm gaps, the negative dc breakdown voltages are lower than the corresponding positive dc breakdown voltages. For all gaps, the negative corona inception voltages are lower than the

corresponding positive corona inception voltages with some minor deviations; no matter if the negative breakdown voltage is higher or lower than the corresponding positive breakdown voltage.

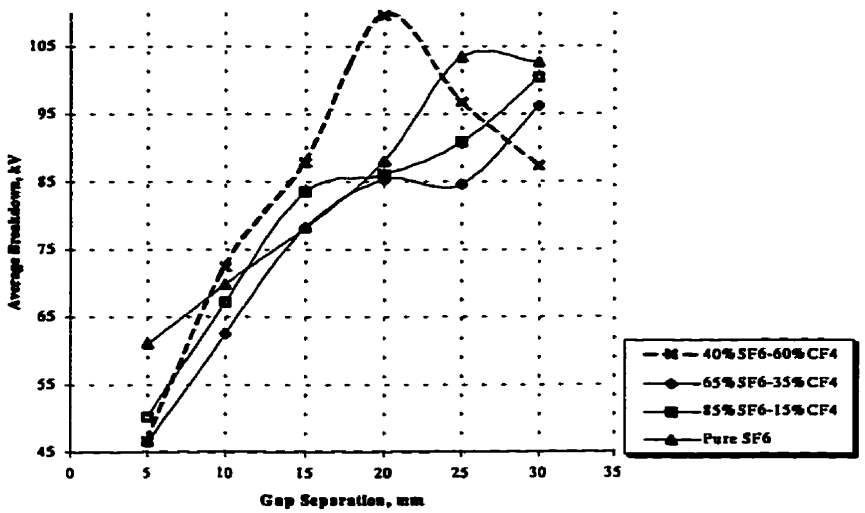

Figure 3.11 Average positive polarity dc breakdown versus gap separation, 300 kPa

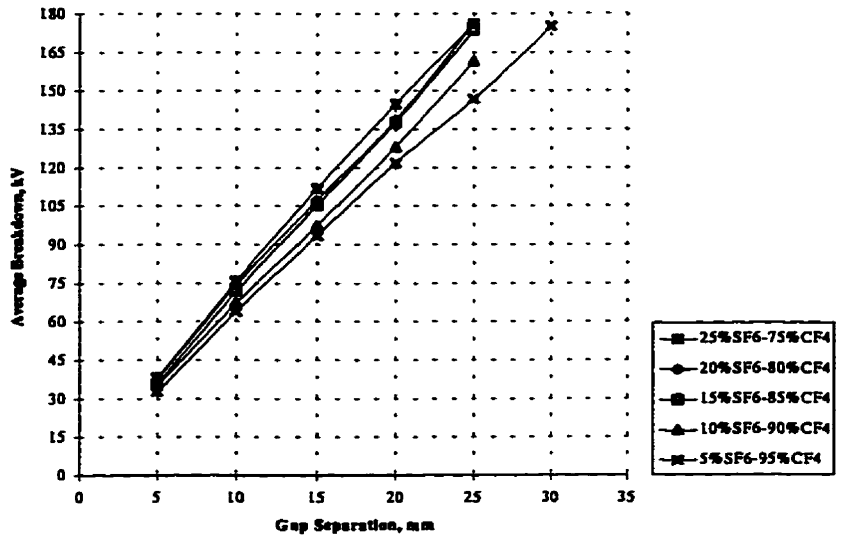

Figure 3.12 Average negative polarity dc breakdown for mixtures with 0-25% SF_6 content versus gap separation, 300 kPa

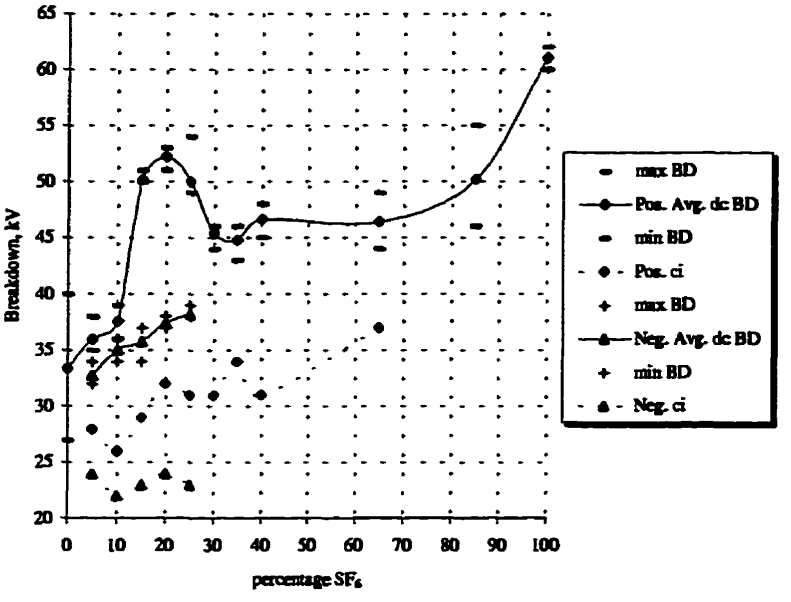

Figure 3.13 Average dc breakdown and corona inception voltages plotted against percentage SF_6 in mixture, 5 mm gap (300 kPa)

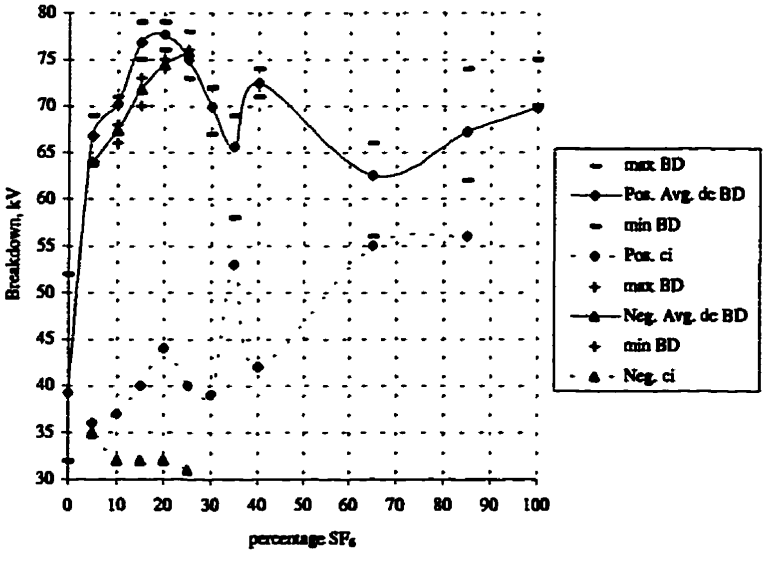

Figure 3.14 Average dc breakdown and corona inception voltages plotted against percentage SF_6 in mixture, 10 mm gap, 300 kPa

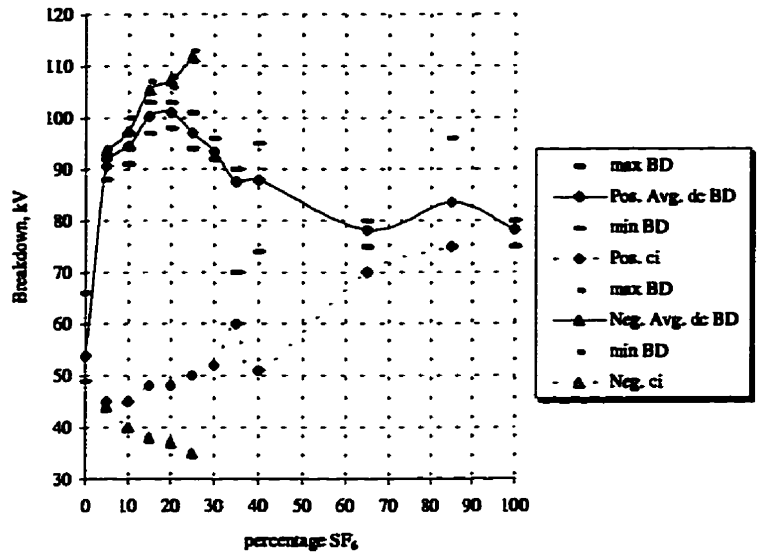

Figure 3.15 Average dc breakdown and corona inception voltages plotted against percentage of SF_6 in mixture, 15 mm gap, 300 kPa

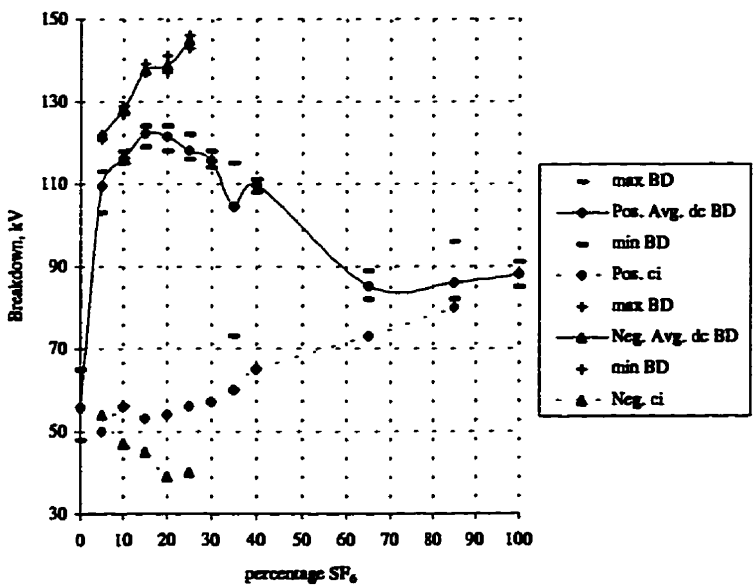

Figure 3.16 Average dc breakdown and corona inception voltage plotted against percentage of SF_6 in mixture, 20 mm gap, 300 kPa

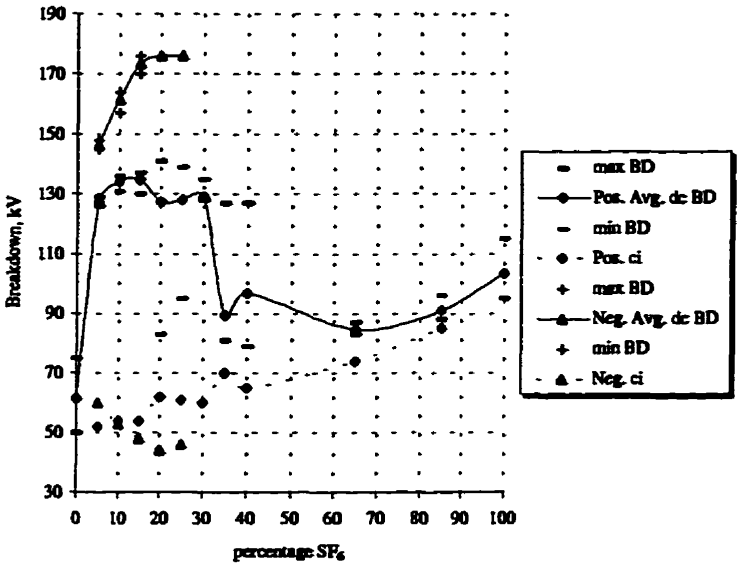

Figure 3.17 Average dc breakdown and corona inception voltages plotted against percentage of SF_6 in mixture, 25 mm gap, 300 kPa

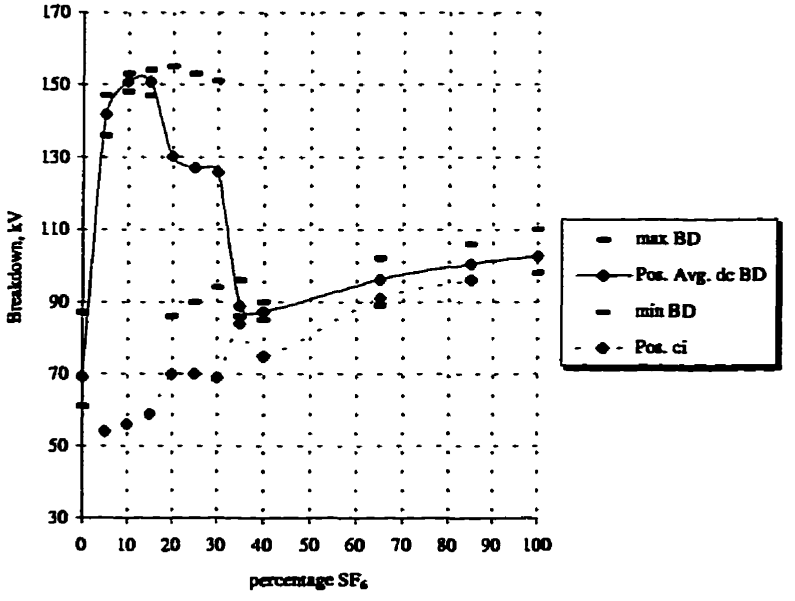

Figure 3.18 Average positive dc breakdown and corona inception voltage plotted against percentage of SF_6 content in mixture, 30 mm gap, 300 kPa

III.a.3 Summary of results on standard lightning impulse breakdown tests

The standard impulse breakdown voltage versus percentage SF_6 content is shown in Figure 3.19. The positive synergism is not evident, especially for the mixtures with SF_6 content of 5-40 percent. There are some isolated instances showing increase of the breakdown voltages for gaps larger than 10 mm toward higher proportions of SF_6 in mixture.

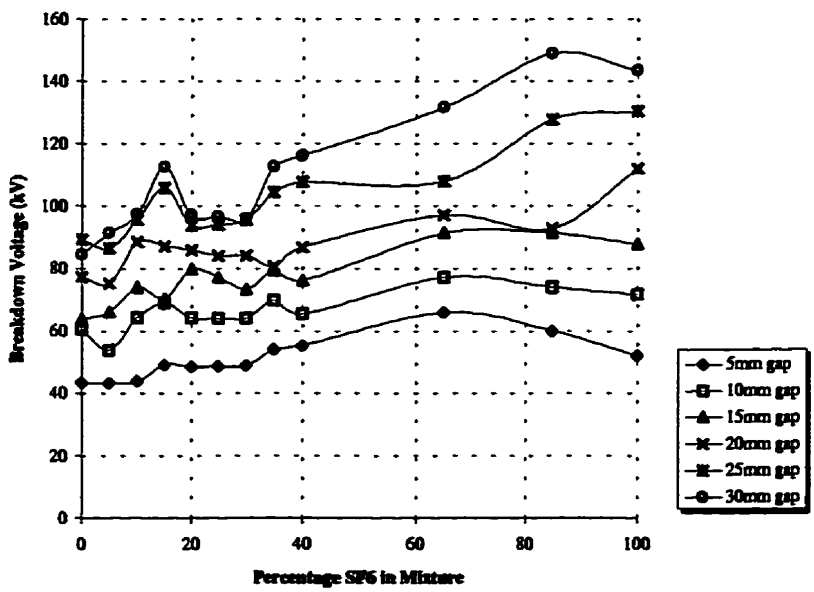

Figure 3.19 50% positive standard impulse breakdown as a function of SF_6 content in mixture, 300 kPa

Figures 3.20-3.22 show positive 50% standard lightning impulse breakdown voltages plotted against gap separation. In Figure 3.20, the mixtures behave erratically; the curves intercept at different points. An increase in 50% breakdown voltage is

observed for 15%SF_6/85%CF_4 mixture at 25mm gap. The same devious trend is noted in Figure 3.21, plus a jump of breakdown voltage at 25 mm gap for 35%SF_6/65%CF_4 and 40%SF_6/60%CF_4 mixtures.

For mixtures with 40, 65 and 85% SF_6 content and pure SF_6 depicted in Figure 3.22, the same erratic behaviour is observed; note that the curve of pure SF_6 increases linearly with increasing gap length. For negative standard lightning impulse breakdown (Figure 3.23), high breakdown voltages and steep and linear slope of increasing breakdown strength are notable.

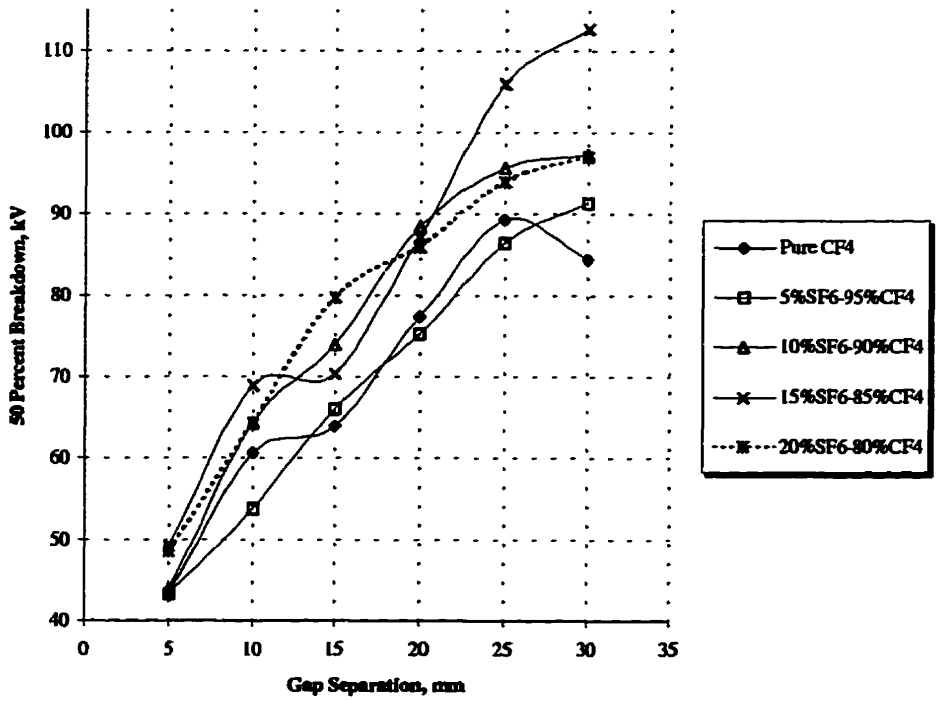

Figure 3.20 50% positive standard lightning impulse breakdown versus gap separation (0-20% SF_6)

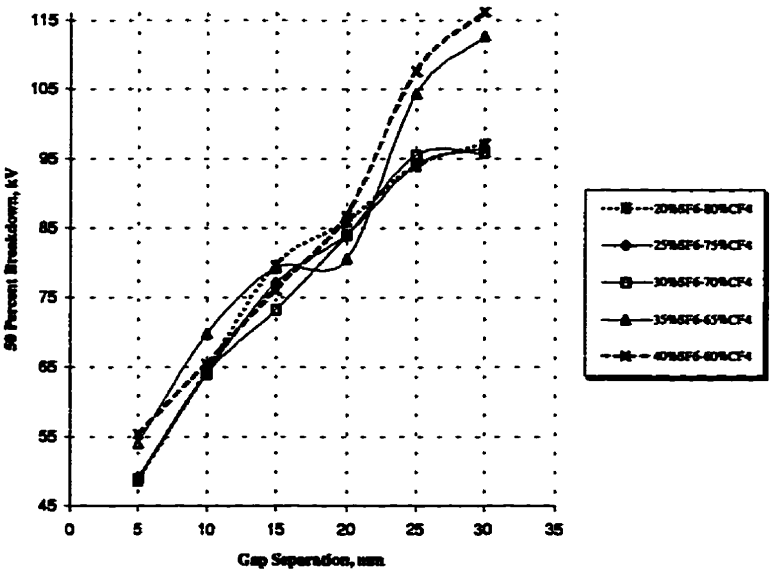

Figure 3.21 50% positive standard lightning impulse breakdown voltage versus gap separation (20-40% SF_6)

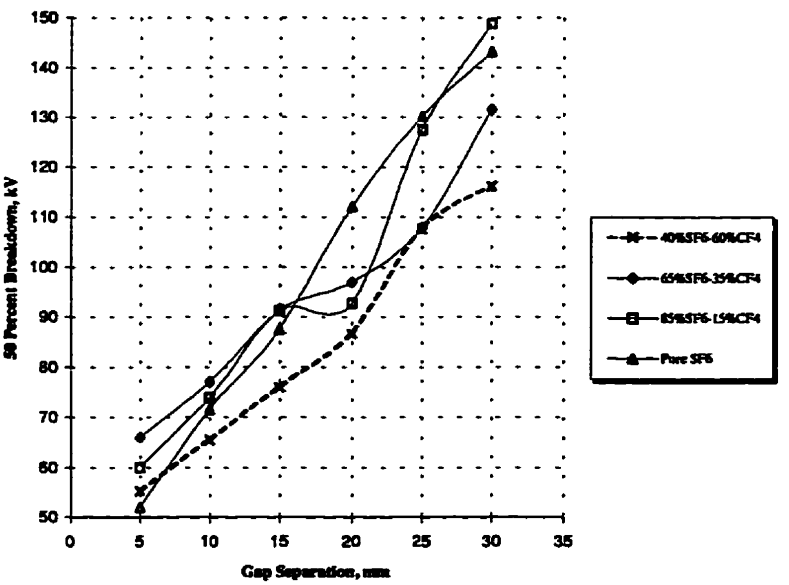

Figure 3.22 50% positive standard lightning impulse breakdown versus gap separation (40-100% SF_6)

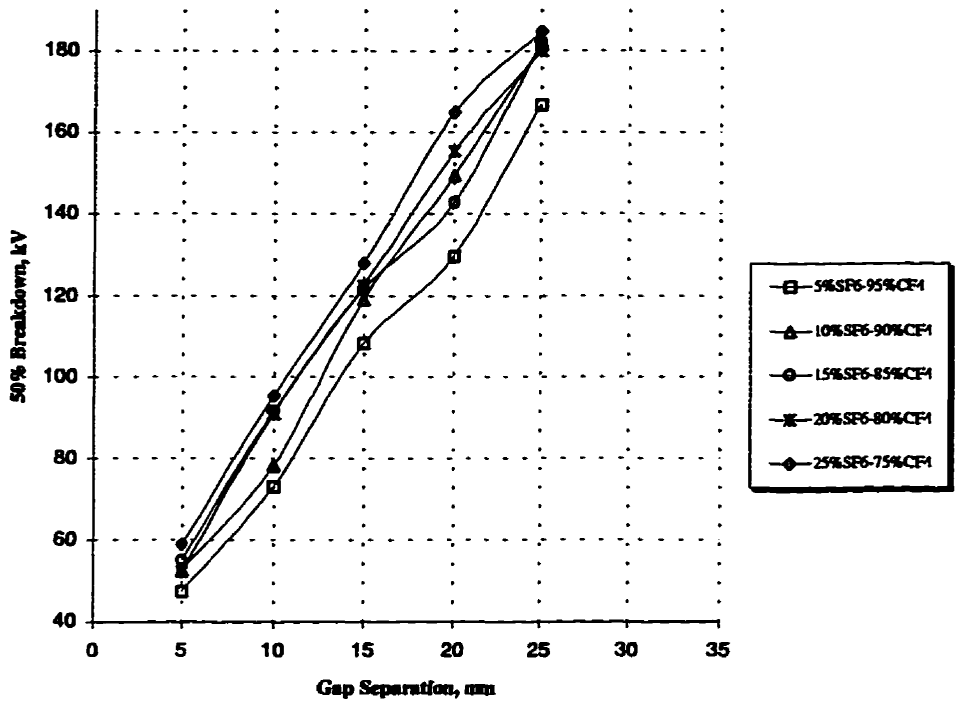

Figure 3.23 50% negative standard lightning impulse breakdown voltage versus gap separation (5-25% SF_6)

III.a.4 Comparing dc, ac(60 Hz) and standard lightning breakdown voltages

Figures 3.24-3.29 are the average ac and positive polarity dc and 50% positive standard lightning impulse breakdown voltages plotted versus the percentage of SF_6 in mixture. They also include corresponding corona inception voltages for ac and positive polarity dc tests. In Figure 3.24 (5 mm gap), average ac breakdown is the lowest with no sign of positive synergism; for dc other than the maximum breakdown voltage in pure SF_6, an increase in breakdown voltage for $20\%SF_6/80\%CF_4$ is noteworthy.

Regarding corona inception, the curves follow the non-uniform field theory applicable to both dc and ac (low corona inception voltage corresponds to higher breakdown, corona stabilization). In Figure 3.25 (10 mm gap), the positive polarity dc breakdown curve rises to a higher level than positive standard lightning impulse curve; the average dc breakdown voltage increase from pure CF_4 to 5%SF_6/96%CF_4 is very steep and the synergistic effect in 5-30% SF_6 content range becomes very noticeable. For dc, higher voltage breakdown points correspond to lower voltage corona points. Contrary to dc, ac corona does not follow the same trend and deviates in the range of 10-40% of SF_6 content. In Figure 3.26 (15 mm gap), the positive synergism for average dc breakdown has become prominent. The ac breakdown voltage shows an initial rapid increase with addition of small amount of SF_6 content similar to dc voltage. No positive synergism occurs for the standard lightning impulse curve at this gap setting. In Figure 3.28, the ac and dc curves show the same degree of positive synergism for 25 mm gap (5-30% SF_6 content per volume). Comparably, the ac corona inception occurs at lower voltage level than dc. Finally for 30 mm gap (Figure 3.29), while ac positive synergism remains high, the dc equivalent starts decreasing; the ac corona inception still remains lower than dc.

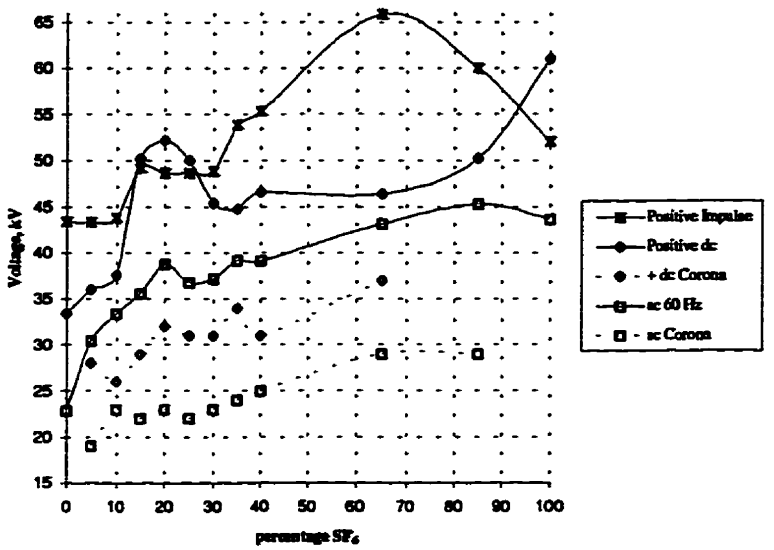

Figure 3.24 Breakdown and corona inception plotted against percentage SF_6 in mixture , 5 mm gap

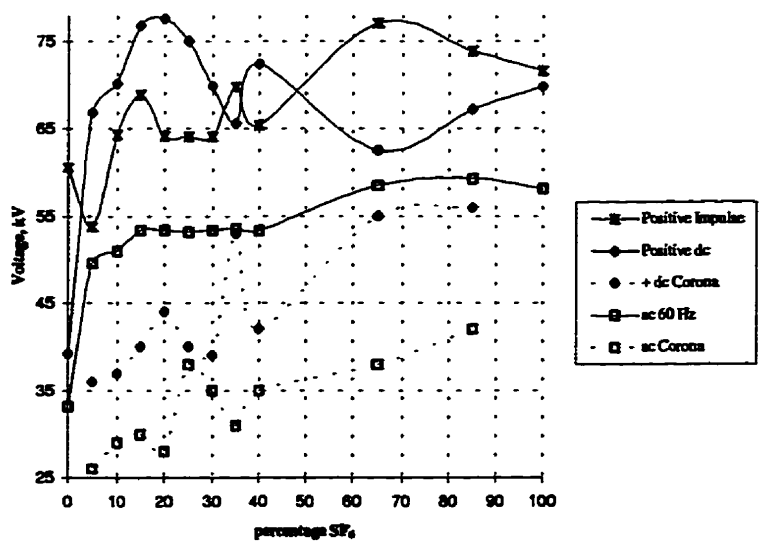

Figure 3.25 Breakdown and corona inception against percentage SF_6 in mixture, 10 mm gap

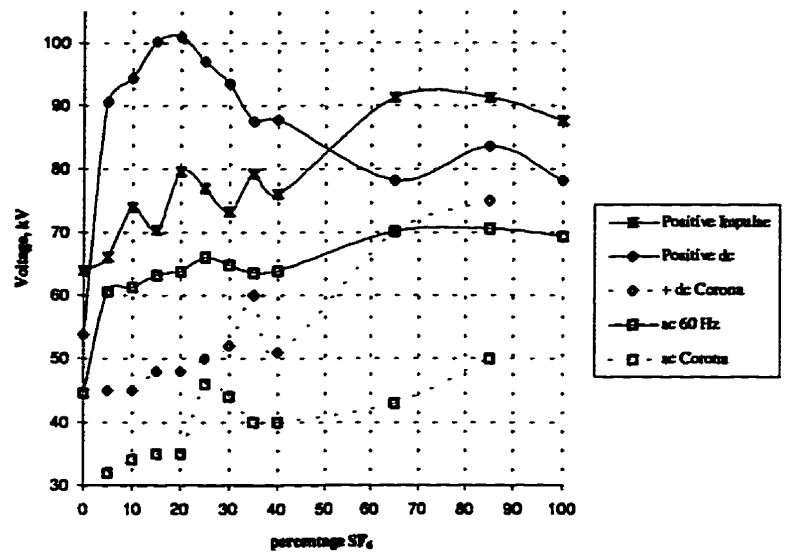

Figure 3.26 Breakdown and corona inception against percentage SF_6 in mixture, 15 mm gap

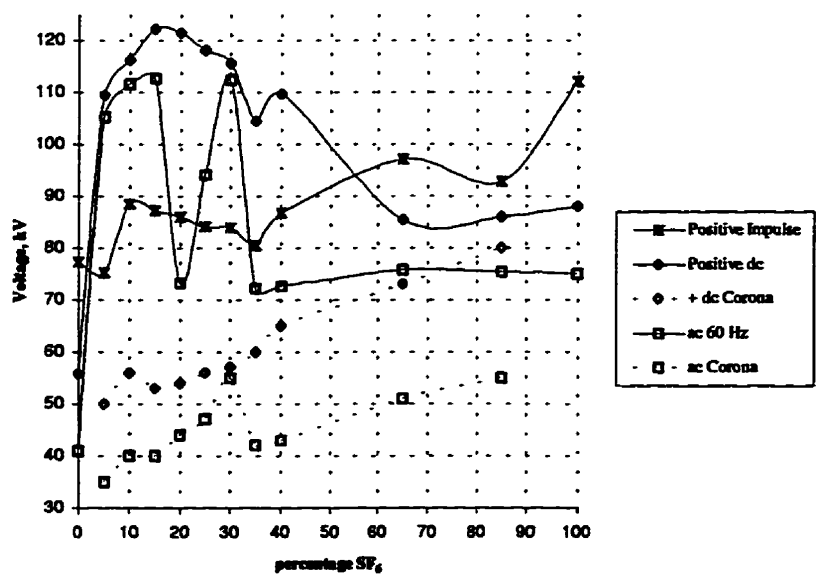

Figure 3.27 Breakdown and corona inception against percentage SF_6 in mixture, 20 mm gap

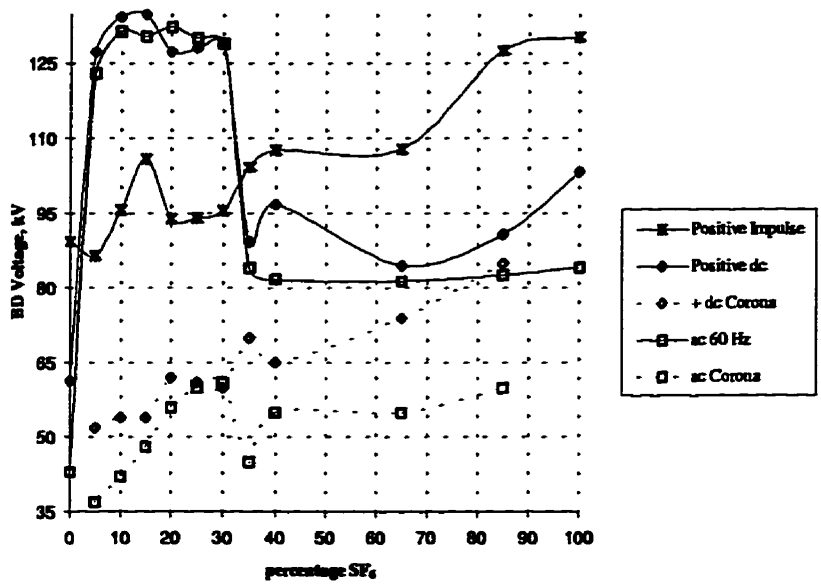

Figure 3.28 Breakdown and corona inception against percentage SF_6 in mixture, 25 mm gap

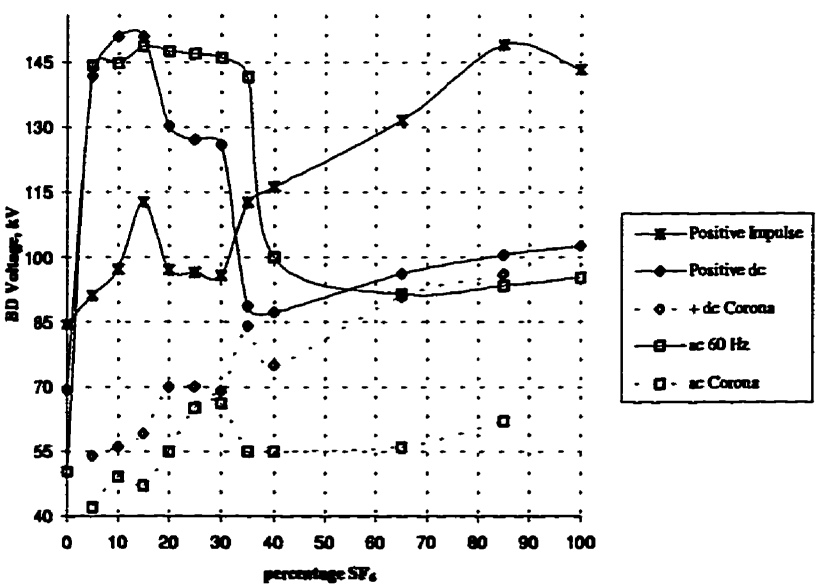

Figure 3.29 Breakdown and corona inception against percentage SF_6 in mixture, 30 mm gap

III.a.5 Time to breakdown results for standard lightning impulse breakdown voltages

Figures 3.30-35 depict the 50% standard lightning impulse breakdown voltages and corresponding average time to breakdowns plotted versus the percentage of SF_6 content per volume in mixture. The following observations have been made.

There exist a general trend that a higher standard lightning impulse breakdown voltage corresponds to a lower average time to breakdown with minor deviations. The average time to breakdown for negative impulse generally shows a lower range of fluctuations than the average time to breakdown for positive impulse. As the gap length is increased (>10 mm), the average times to breakdown for different mixtures fall into a narrower range or band of fluctuation. For gaps larger than 10 mm, this band is approximately 2 microseconds wide; for 5 and 10 mm gaps, it is wider than 3 microseconds. Finally, majority of the average time to breakdown points fall below 5 microseconds (for all gap lengths).

Next is the volt-time characteristics of mixtures in the region with the strongest positive synergism. Figures 3.36-3.43 show the positive and negative polarity volt-time characteristics for mixtures with 5-20% SF_6. These volt-time characteristics display differences. Referring to Figures 3.36 and 3.37, the points of negative volt-time characteristic are more spread than the positive volt-time characteristics for $5\%SF_6/95\%CF_4$ mixture. The range of variation of time to breakdown for negative impulse is approximately 2-6 microseconds while for positive impulse is 2-4 microseconds. The converse is true for $20\%SF_6/80\%CF_4$ mixture; referring to Figures

3.42 and 3.43, the negative volt-time points are densely distributed in a region 1 microsecond wide as opposed to the positive volt-time which is distributed over a region of at least 5 microsecond wide. For mixtures with 15%SF_6/85%CF_4 content, a broader scatter of points is observed for positive volt-time characteristics. However, both positive and negative volt-time characteristics are denser (more points) for shorter times to breakdown (2-4 microseconds). Finally, referring to volt-time characteristics of 10%SF_6/90%CF_4 mixture, we observe larger scatter for longer gaps; this scatter is wider for positive volt-time characteristics (Figures 3.38 and 39).

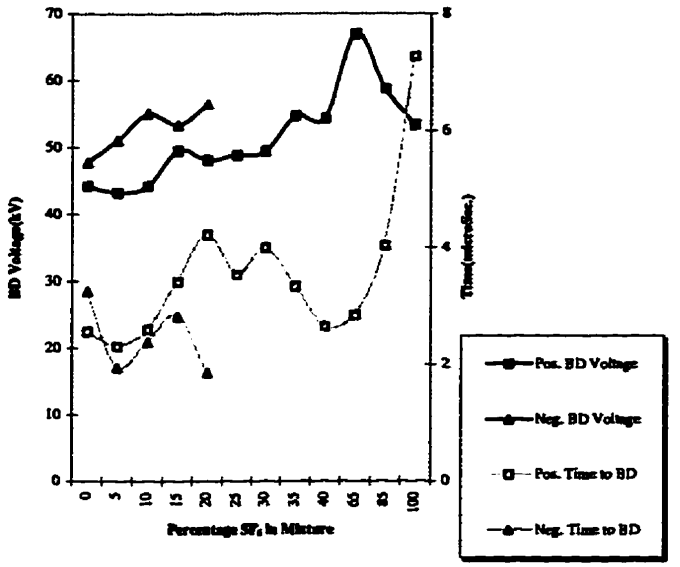

Figure 3.30 50% Standard lightning impulse breakdown and corresponding average time to breakdown plotted versus percentage SF_6 in mixture, d=5mm (300 kPa)

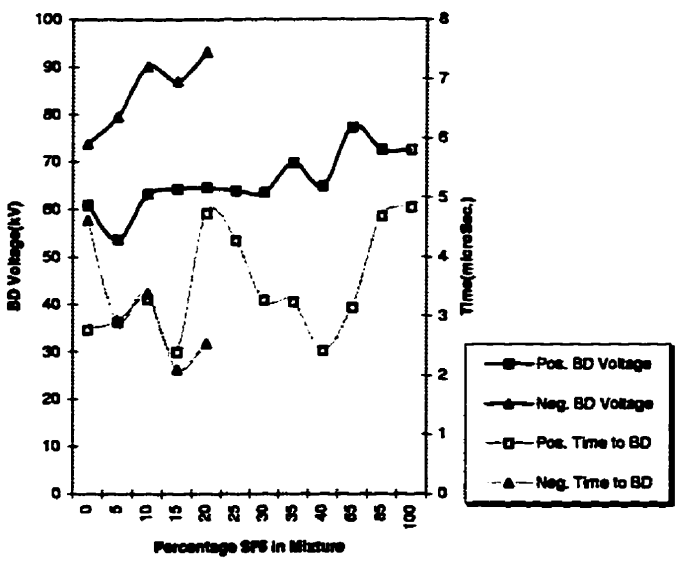

Figure 3.31 50% Standard lightning impulse breakdown and corresponding average time to breakdown plotted versus percentage SF_6 in mixture, d=10mm (300 kPa)

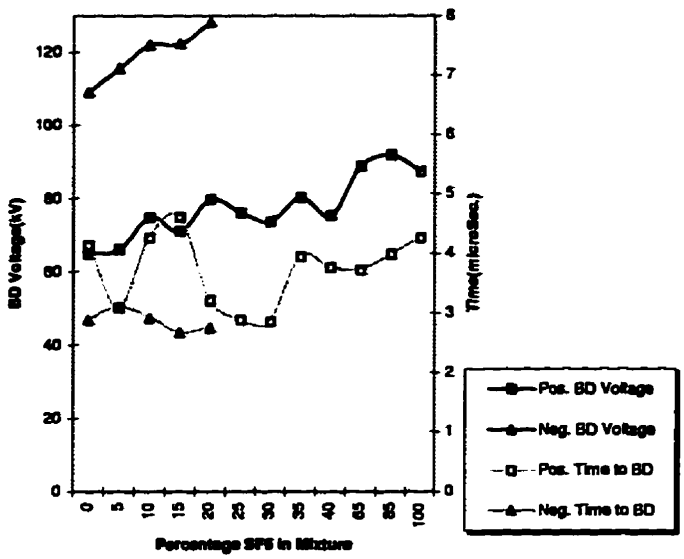

Figure 3.32 50% Standard lightning impulse breakdown and corresponding average time to breakdown plotted versus percentage SF_6 in mixture, d=15mm.(300 kPa)

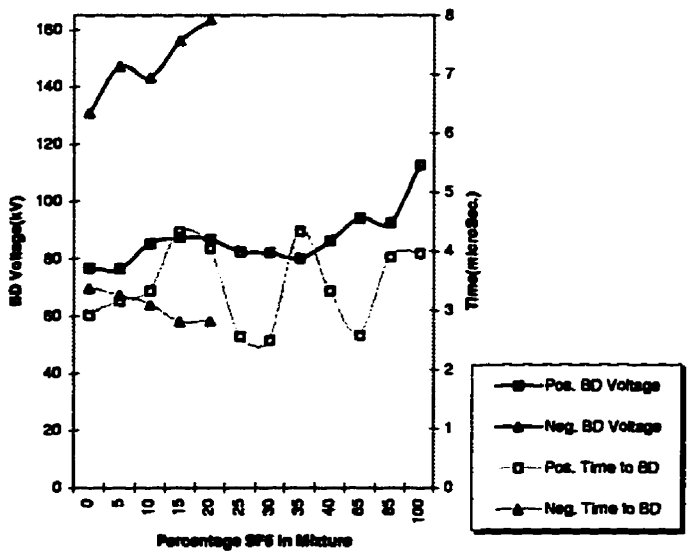

Figure 3.33 50% Standard lightning impulse breakdown and corresponding average time to breakdown plotted versus percentage SF_6 in mixture, d=20mm (300 kPa)

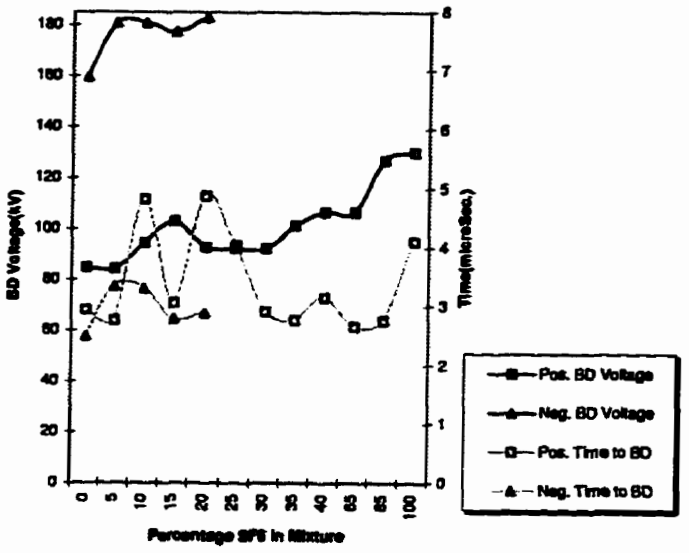

Figure 3.34 50% Standard lightning impulse breakdown and corresponding average time to breakdown plotted versus percentage SF_6 in mixture, d=25mm (300 kPa)

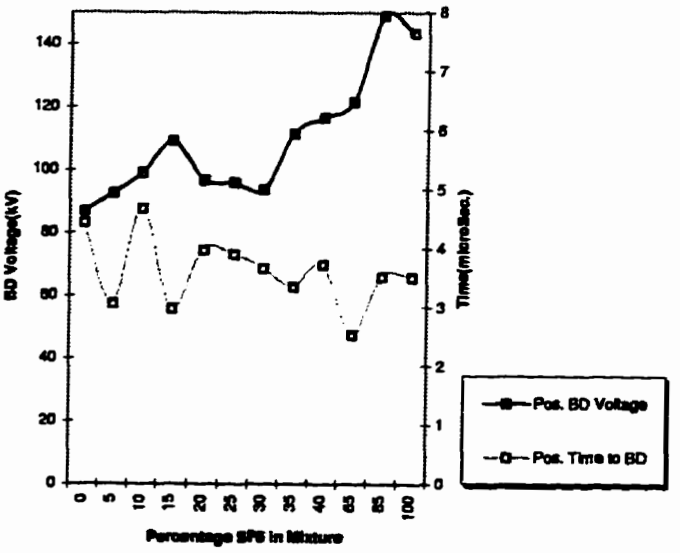

Figure 3.35 50% Standard lightning impulse breakdown and corresponding average time to breakdown plotted versus percentage SF_6 in mixture, d=30mm (300 kPa)

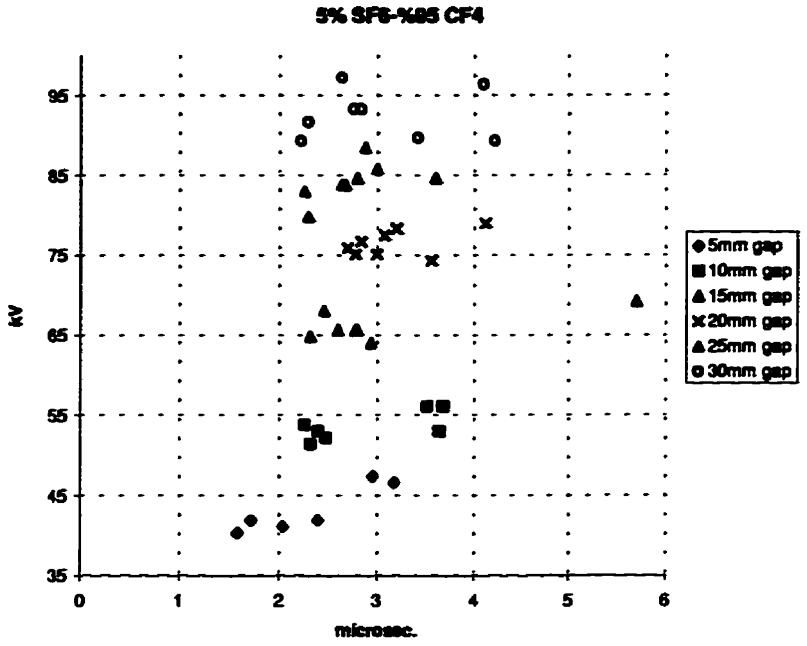

Figure 3.36 Volt-time characteristics for positive lightning impulse breakdown for mixtures with proportion $5\%SF_6/95\%CF_4$ at 300kPa

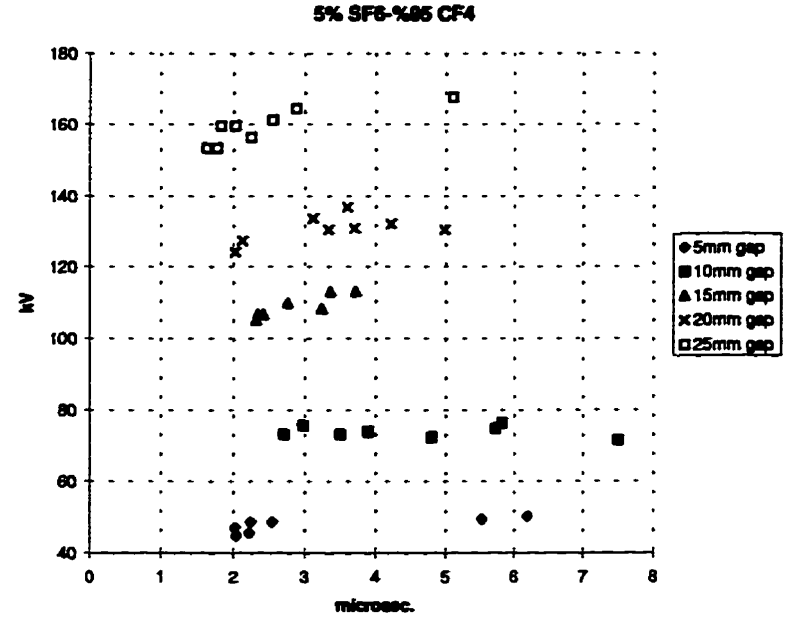

Figure 3.37 Volt-time characteristics for negative lightning impulse breakdown for mixtures with proportion $5\%SF_6/95\%CF_4$ at 300kPa

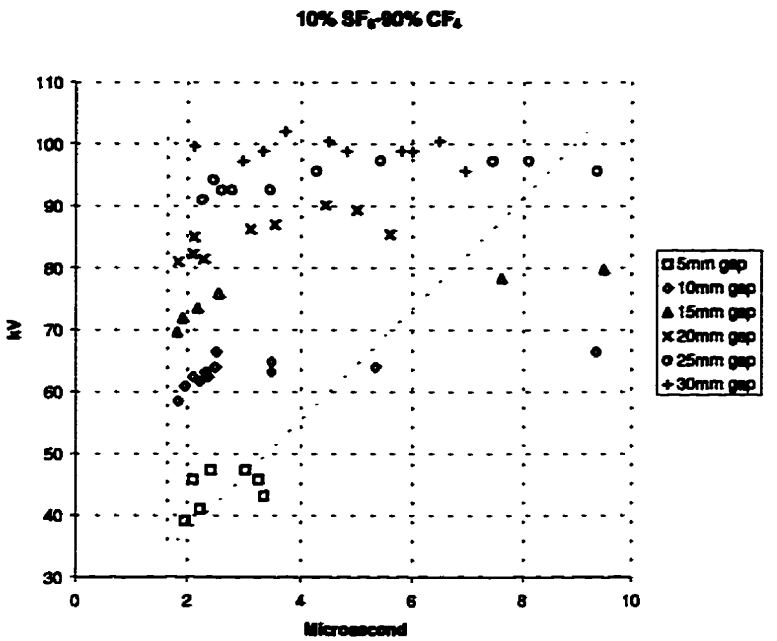

Figure 3.38 Volt-time characteristics for positive lightning impulse breakdown for mixtures with proportion $10\%SF_6/90\%CF_4$ at 300kPa

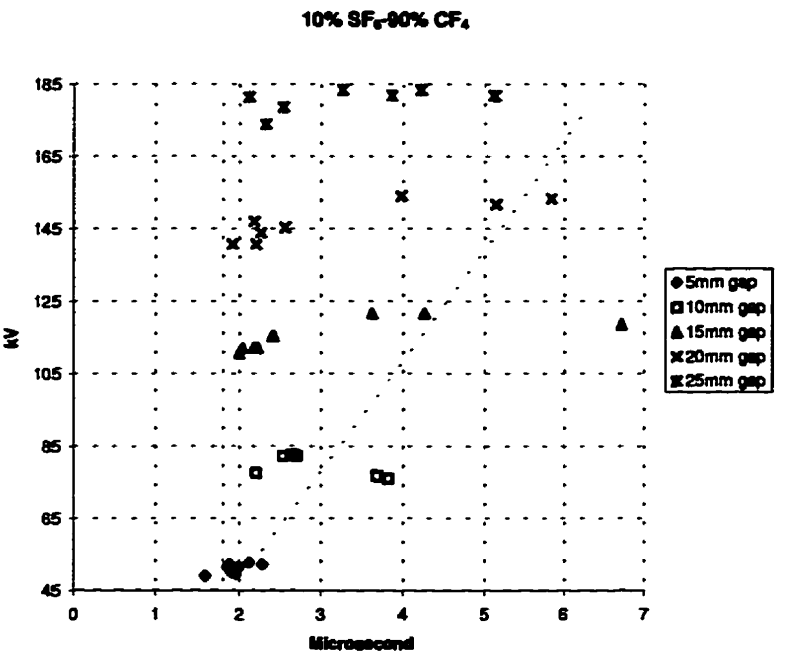

Figure 3.39 Volt-time characteristics for negative lightning impulse breakdown for mixtures with proportion $10\%SF_6/90\%CF_4$ at 300kPa

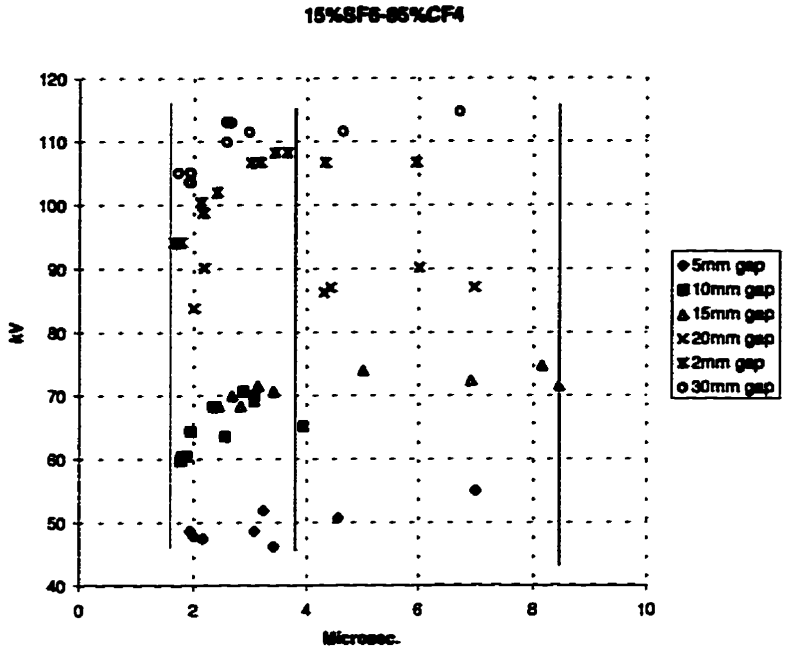

Figure 3.40 Volt-time characteristics for positive lightning impulse breakdown for mixtures with proportion $15\%SF_6/85\%CF_4$ at 300kPa

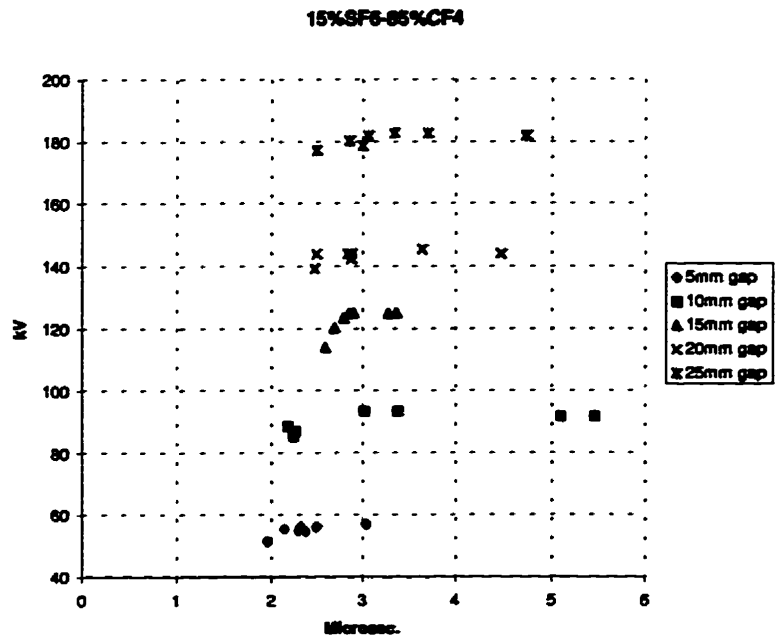

Figure 3.41 Volt-time characteristics for negative lightning impulse breakdown for mixtures with proportion $15\%SF_6/85\%CF_4$ at 300kPa

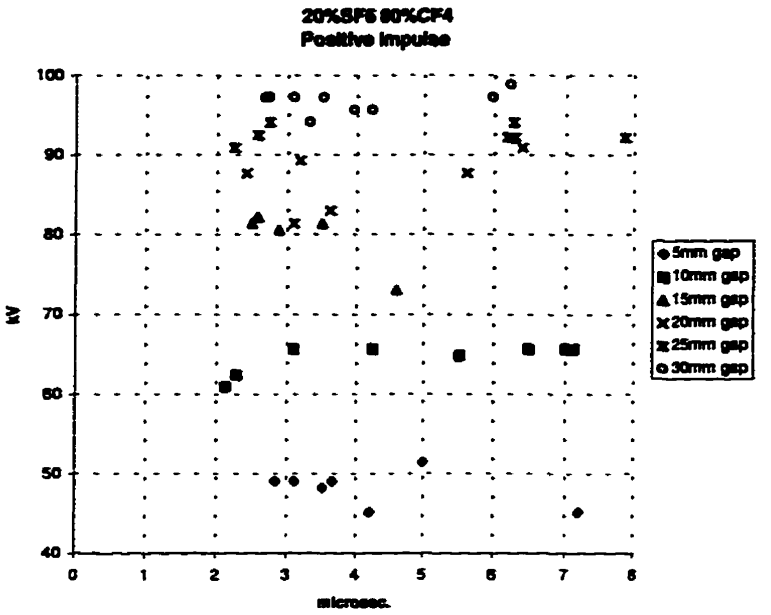

Figure 3.42 Volt-time characteristics for positive lightning impulse breakdown for mixtures with proportion $20\%SF_6/80\%CF_4$ at 300kPa

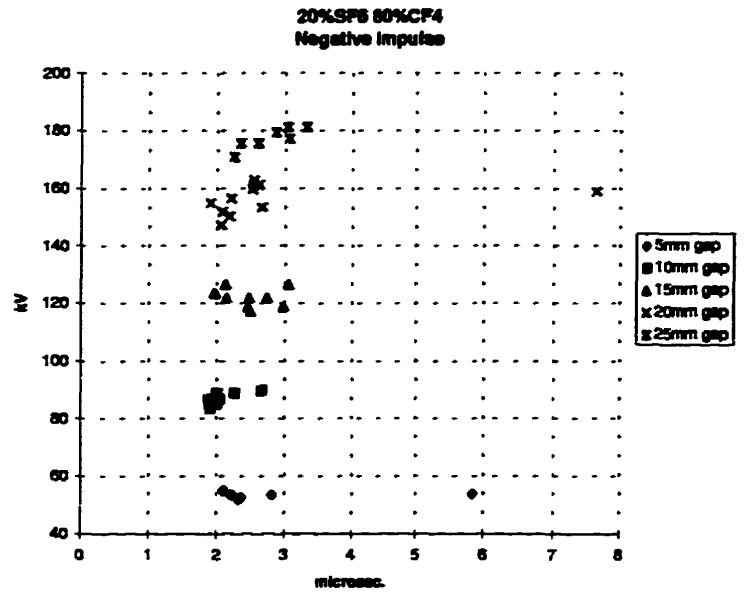

Figure 3.43 Volt-time characteristics for negative lightning impulse breakdown for mixtures with proportion $20\%SF_6/80\%CF_4$ at 300kPa

III.b Discussion

In the recent study, Berg [14] noted a large positive synergistic effect for ac (60 Hz) and positive polarity dc breakdown of SF_6/CF_4 mixtures in non-uniform fields. Large increases in breakdown strength were observed starting in mixtures with 10% SF_6 content per volume. Furthermore, ac test results showed higher breakdown voltages than the corresponding dc test results; possibly, due to particle accumulation inside the test chamber under application of dc voltage. [14]

Positive standard lightning impulse voltages did not show the same trend; 100% SF_6 breakdown versus gap distance defined the upper limit of breakdown for the lightning impulse, whereas for positive polarity dc the 100% SF_6 breakdown lied between the 100% CF_4 breakdown and the mixtures of SF_6-CF_4. The lightning impulse showed a relatively linear relationship for all gaps (10,20,25,30mm) for mixtures containing more than 10% SF_6. [14]

According to Berg, the positive synergism for dc and ac test was most pronounced for ≈25%SF_6-75%CF_4 mixtures for all gap lengths. For both 10 and 25mm gaps, a significant increase in breakdown strength was observed after addition of the first 10% of SF_6 to CF_4 (≈65kV increase in breakdown strength while the breakdown voltage plotted against percentage SF_6 in mixture). [14]

The present research also validated a steep increase in breakdown voltage for ac and dc voltages, starting in mixtures with 5% SF_6 per volume (Figures 3.1 and 3.8). This study focused at mixtures with 5-40% SF_6 content, the SF_6 content was increased in 5%

steps each time. All mixtures in this range were investigated with respect to, breakdown voltage and corona inception voltage for dc and ac, and breakdown voltage and time to breakdown for standard lightning impulse.[1]

As in Berg's work, the positive synergism was not observed under standard lightning impulses (Figure 3.19). For standard lightning impulse, the maximum breakdowns occurred near 100% SF_6 content. One possible explanation of the observed difference may be the lack of sufficient time for the establishment of space charges which modifies the distribution of the field near the electrodes. Space charge fields play an important role in the mechanism of corona and spark development in non-uniform field gaps [27]. Sufficient time for establishment of space charges is available under ac and dc voltages; when the voltage is applied for a long time, the ionization products will have sufficient time to wander in the gap and accumulate in space, causing a distortion in the original field [26]. For ac and dc, as the field becomes increasingly divergent (longer gap in point-sphere arrangement); the synergistic effect of SF_6/CF_4 mixtures becomes more prominent.

In non-uniform field gaps, all evidence suggest that a strong field dependent electron production must be present. In electrically stressed electronegative gases, the major source of breakdown initiating free electrons is electron detachment from the negative ions and therefore, occurs with highest probability in the vicinity of positively stressed electrode under non-uniform field condition. The detachment process is mostly collisional rather than electric field induced. On the other hand, electric field induced

[1] Note that Berg did not investigate 5%SF_6/95%CF_4 mixtures.

electron detachment is an unlikely source of initiatory electrons in gas-insulated systems unless negative ions with very small electron energies exist in the field region [28,29].

CF_4 has high electronegative property for higher electron energies (typically ≥ 2.5eV). As field becomes more divergent, the electrons because of their high mobility are drawn towards the positive point and ionization by electron collision takes place in the high field region close to the point. As the electrons drawn towards the anode (point), the positive space charge left behind causes a reduction in the field strength close to the point while at the same time increasing the field further away from it. As space charge propagates further into the gap, the field strength at the tip of the space charge may be high enough to initiate a cathode-directed streamer which in SF_6 or CF_4 alone would lead to breakdown of the gap. However, for SF_6/CF_4 mixtures, it appeared that the electronegative CF_4 molecules might trap some of the high energy electrons thus greatly reducing the probability of breakdown [26,14]. It is also possible that electron detachment from CF_4 molecules reduces the field strength further away from the positive point; in other words, the electron detachment from CF_4 facilitates the corona stabilization of the gap against streamer breakdown.

For negative polarity dc and mixtures with 5-25% SF_6 content (Figure 3.12), very rapid increase in breakdown voltages were noted as gap length increased. With the negative point, the electrons are repelled into the low field region and become attached to the SF_6 and CF_4 molecules. They tend to hold back the positive space charge which remains in the space between the negative charge and the point. In the vicinity of the

point the field is grossly enhanced, but the ionization region is drastically reduced. CF_4 molecules are capable to trap free electrons with higher energy in this region and further contribute to the retarding action of the space charges. Finally, the applied field sweeps away the negative and positive ion space charge from the point and the cycle starts again after the clearing time for the space charges. The net effect is a higher breakdown voltage needed to overcome the retarding action of ions. Since, the most prominent factor impeding the initiation of the breakdown is not the electronegative property of CF_4 molecules and a stronger mechanism prevails; there is an overall low probability of streamer breakdown and the negative breakdown strength increases linearly with gap length.[26]

For mixtures with 5-25% SF_6, the breakdown voltage values for negative dc and 5 and 10 mm gaps were lower than the comparable breakdown voltage values for positive dc. However, for larger gaps the negative dc breakdown voltages were appreciably higher than the positive dc breakdown voltages. The corona inception voltages remained lower than their positive equivalents (Figures 3.13-3.18). Under negative point electrode, the electrons are repelled into the low field region between electrodes. They are normally attached to SF_6 and CF_4 molecules and hold back the positive space charge which remains in the space between the negative charge and the point, causing enhancement of the field in the vicinity of the point while reducing the ionization region.[26] Possibly, due to short gap length and high field, the repelled electrons possess high energy and the electronegative SF_6 and CF_4 molecules can not capture

them effectively. These high energy electrons detach more electrons from the gas molecules by collision in the high field region near the point; under high field condition, this rapidly gives rise to a cathode-directed streamer breakdown. For longer gaps, the field close to the point electrode is not as high as that of shorter gaps; besides the repelled electrons from the negative point are captured effectively by gas molecules; the space charge regions between two electrodes are formed and the retarding action of ions summed with affinity of CF_4 for high energy electrons produce a high negative dc breakdown strength.

For positive dc breakdown, the region of positive synergism for all gaps corresponds to an early initiation of corona (Figures 3.13-3.18). For a positive point, more electrons are generated by collision in the high field region near the point. The electrons are drawn into the point; the positive space charge created by electron deficiency near the point, will reduce the field strength close to the point and will increase the field strength further away. It is speculated that the presence of CF_4 molecules close to the point, facilitate the production of the electrons by detachment; this gives rise to an early corona inception. The corona near the point, changes the distribution of the space charge in the region which in turn stabilizes the gap against an early cathode-directed streamer. The result will be a higher breakdown voltage for the non-uniform field arrangement and consequently, the positive synergism shows up for the gas mixture.

The 60 Hz ac breakdown voltages did not display positive synergism for gaps shorter than 20mm (Figure 3.1). But for 20-30mm gaps, the ac positive synergism

approaches the breakdown voltage values even higher than the comparable positive dc voltage values (Figures 3.24-29). During the negative half cycles, there is a high probability of breakdown due to initiation of a cathode-directed streamer caused by the enhanced field in region near the negative point electrode and enhanced electron detachment by collision. During positive half cycles, the high field region located further away from the positive point and the formation of the space charge regions may contribute to low breakdown strength and absence of positive synergism for the gas mixture. For longer gaps, the electronegative CF_4 molecules work effectively to trap high energy electrons; also, an early inception of corona helps stabilizing the gap against an early cathode-directed streamer breakdown. Considering the net effect of actions happening during each half cycle, stronger retarding actions affecting deionization during negative half cycles summed with the positive half cycle retarding events contributes to the lower ac breakdown for shorter gaps. Conversely for long gaps, the sum of actions promoting deionization during two half cycles occasionally boosts the ac breakdown strength higher than its positive dc counterpart. The formation of conductive paths caused by particle accumulation under constant dc voltage, is another probable factor causing occasional drop in positive dc breakdown voltage.

In a non-uniform field, large scatter in time lags exist and the results fall into a dispersion band. Long and highly scattered time lags are observed for strongly electronegative gases. For SF_6 and other electronegative gases, the long time lags are associated with the complex nature of the spark growth mechanism.[26] The average

time to breakdown values for negative standard lightning impulse voltages are generally shorter than those for positive impulse breakdowns (Figures 3.30-35). Note that, the negative standard lightning breakdown voltages are considerably higher than the positive impulse counterparts. The short negative impulse time lags are probably due to the enhanced field region near the negative point electrode. Applying a sufficiently high negative lightning impulse, the extremely high field is formed; the streamers will develop rapidly when the retarding action of space charges can not support the gap against breakdown.

Referring to Figures 3.38 and 3.39, shorter gaps show smaller scatter of time lags while longer gaps show larger scatter. This probably happens due to the increasing field non-uniformity, which in turn contributes to more complex corona stabilization and breakdown mechanisms. For shorter gaps, the breakdown may be initiated by development of streamers and hence showing much shorter time lags.

IV. Conclusion

The following summarizes the important observations made during the present studies of breakdown characteristics of SF_6/CF_4 gas mixtures in highly non-uniform fields:

– A steep increase in breakdown voltage was observed for ac and dc voltages, starting with mixtures of 5% SF_6 per volume. The increase in breakdown voltage continued up to the mixtures with 35% SF_6 per volume (positive synergism). As field became increasingly divergent (longer gaps), the synergistic effect of SF_6/CF_4 mixtures became more prominent.

– Very high and linearly rising breakdown voltages versus increasing gap length were noted for negative dc voltage and mixtures with 5-25% SF_6 content per volume.

– For mixtures with 5-25% SF_6, the breakdown voltage values for negative dc and 5 and 10mm gaps were lower than the comparable voltage values for positive dc. However, for larger gaps the negative dc breakdown voltages became appreciably higher than the positive dc breakdown voltages.

– The 60 Hz ac breakdown voltages did not display positive synergism for gaps shorter than 20mm. For 20-30mm gaps, the ac positive synergism approached the breakdown voltage values higher than the comparable positive dc voltage values.

– Under positive dc voltages, the region of positive synergism for all gaps corresponded to an early initiation of corona.

– The ac corona inception occurred at lower voltage levels than dc.

– A higher lightning impulse breakdown voltage corresponded to a lower average time to breakdown and vice versa.

– The average time to breakdown corresponding to negative lightning impulse breakdown voltages are generally shorter than those of positive impulse voltages.

– The average time to breakdown for negative impulse breakdown voltages generally were less scattered.

– For positive lightning impulse tests, as the gap length is increased above 10mm the average time to breakdown for various mixtures also fell into a narrow band.

The desirable dielectric properties of SF_6/ CF_4 mixtures seem to be promising in future high-voltage gas-insulated apparatus provided that, the ban on wrongfully labeled CF_4 is removed.

References

1. H. Moissan and P. Lebeau, Component Review, Vol. 130, p. 180, 1900.

2. F. Cooper, "Gas Insulated Devices", US Patent No. 2221670, 1940.

3. V. Maller and M. Naidu, "Advances in High Voltage Insulation and Arc Interruption in SF_6 and Vacuum", Ch. 1-2, Pergamon ress, Oxford, England, 1981.

4. F. M. Clark, "Insulating Materials for Design Engineering Practice", Wiley, New York, 116, 1962.

5. T. Anderson, Paper No. 57-82 presented at the meeting of the *American Inst. of Electrical Engrs.* (1957).

6. V. N. Maller and M. S. Naidu, *proc. I. E. E., 133,* 107 (1976).

7. T. Nita, Y. Shibuya, *proc. IEEE Trans. on P.A.S., PAS-90,* 1065 (1971).

8. H. Raether, "Electron Avalanches and Breakdown in Gases", Butterworths, London, 1964.

9. T. Takuma *et al., Proc.I.E.E., 119,* 927 (1972).

10. Von Gerhard Frind, I. Agnew Physik, 12, No.5, 231 (1960).

11. Sulphur hexafluoride, Pennsylvania Salt Company (U. S. A.) Manual SF-1 (1948).

12. D. R. James, "Group Discussion on Requirements of Gas Mixtures for Power Transmission and Distribution Lines", *4th International Symposium on Gaseous Dielectrics*, Konxville, Tenn., 1984.

13. D. W. Bouldin, and Colleagues, "A Current Assessment of the Potential of Dielectric Gas Mixtures for Industrial Applications", *Atomic, Molecular & High Voltage Physics Group, Oak Ridge national Laboratory, Oak Ridge, Tennessee,* 4th International Symposium on Gaseous Dielectrics, Konxville, Tenn., 1984.

14. J. M. Berg, "Experimental Studies of SF_6-CF_4 Mixtures for Use as Gaseous Dielectrics in Power System Applications" *Msc. Thesis, Dept of Electrical and Computer Engineering, University of Manitoba*, Winnipeg, Canada, 1995.

15. S. J. Dale, R. E. Wootton and A. H. Cookson (1980). In L. G. Christophorou (Ed.), Gaseous Dielectrics II. Pergamon Press, New York. pp. 256-265.

16. M. O. Pace, C. C. Chan and L.G. Christophorou (1979). IEEE Publication 79Ch1399-5PWR, pp. 168-177.

17. M. O. Pace and Colleagues, "Particle Contamination in Gas-insulated Systems: New Control Methods and Optimum SF_6/N_2 Mixtures", *Atomic, Molecular & High Voltage Physics Group, Oak Ridge national Laboratory, Oak Ridge, Tennessee,* 4th International Symposium on Gaseous Dielectrics, Konxville, Tenn., 1984.

18. D. W. Bouldin, "Group Discussion on Requirements of Gas Mixtures for Transformers and Circuit Breakers", 4th International Symposium on Gaseous Dielectrics, Konxville, Tenn., 1984.

19. L.G. Christophorou, M. O. Pace (Edited by), "Proceeding of the 4th International Symposium on Gaseous Dielectrics", Knoxville, Tennessee, U.S.A., 1984.

20. R. Middleton, V. Koshik, P. Hogg, P. Kulkarni and H. Heiermeirer, "Development Work for the Application of 245 kV Circuit Breakers Using a SF_6-CF_4 Gas Mixture on the Manitoba Hydro System", CEA Conf., Toronto-Canada, March, 1994.

21. G. Camilli, T. Liao and R. Plump, "The Dielectric Behaviour of Some Fluorogases and Their Mixtures", AIEE Trans. Vol. 74, Part I, pp.637-642, 1955.

22. G. Camilli and R. Plump, "Fluorine Containing Gaseous Dielectrics", AIEE Trans., Vol. 72, Part I, pp.93-102, 1953.

23. F. Clark, "Insulating Materials for Design and Engineering Practise", John Wiley and Sons Inc., New York, U.S.A., 1962.

24. Guide on High-voltage Testing Techniques, *[IEC title: High-voltage Test Techniques Part 2. Test Procedures]*, BS 923: Part2: 1980, IEC 60-2: 1973, published by: BSI (British Standards Institution).

25. Guide on High-voltage Testing Techniques, *[IEC title: High-voltage Test Technique, Part4. Application Guide for Measuring Devices]*, BS 923: Part4: 1980, IEC 60-4: 1977, published by: BSI (British Standards Institution).

26. E.Kuffel and W. S. Zaengl, High-voltage Engineering *Fundamentals,* Ch 5, Pergamon Press, 1984

27. L. G. Christophorou and L. A. Pinnaduwage, "Basic Physics of Gaseous Dielectrics"; *Atomic, Molecular & High-Voltage Physics Group, Oak Ridge national Laboratory, Oak Ridge, and Dept. of Physics, The University of Tennessee, Knoxville Tennessee;* IEEE Transaction on Electrical Insulation, Vol.25 No.1, Feb. 1990.

28. H. C. Schweinler and L. G. Christophorou, *Gaseous Dielectrics*, L. G. Christophorou, ed., Vol.2, pp.12-23, 1980.

29. L. G. Christophorou, "Electron Attachment and Detachment Processes in Electronegative Gases", Plasma Physics, Vol.27, pp. 231-281, 1987.

Appendix A

Gas Filling Procedure[1]

[1]Taken from: "Experimental Studies of SF_6-CF_4 Mixtures for Use as Gas Dielectrics in Power System Applications" by Berg J. M., Msc. E.E. Thesis, University of Manitoba, Winnipeg, Canada, May 1995

Because the dielectric strength of a particular gas mixture can vary substantially with an incremental change in the volumetric proportions of the individual constituents, great care must be taken when administering a mixture into a pressure vessel to ensure high accuracy is maintained. As was mentioned in section II.c., a Matheson pressure gauge with a measuring error of ±0.25% was used during the chamber filling process. For any particular test, after the chamber had been evacuated to 0.0013 kPa (≈0.01 mm Hg), the smallest constituent gas was administered first, followed by the larger constituent gas.

For example, suppose a 25% SF_6- 75% CF_4 mixture at 200 kPA (≈29 psig) was required. SF_6 would be first administered into the chamber (after purging all air out of the pressure lines) until the gauge pressure reads 50 kPa. CF_4 would next be administered into the chamber until the gauge pressure reads 200 kPa. Prior to any testing, the mixing fan inside the chamber would be activated and the gases allowed to mix for at least one hour. After completion of testing for a particular mixture, suppose it is required to perform testing on a 50% SF_6- 50% CF_4 mixture. Instead of purging the chamber and administering a new mixture which would not only be time consuming but very wasteful of gases (recommended for precise results if resources are available), the following procedure was followed which minimizes the conservation of gas supplies and minimizes the amount of the down time.

Step 1: Calculate individual gas proportions based on the total pressure[2].

[2] Dimensions used for all pressure calculation were pounds per square inch gauge (psig)

29.00755= 7.25189+ 21.75566

Step 2: For a resulting mixture of 50% SF_6- 50% CF_4, the new pressure of SF_6 must increase to 14.50377 from 7.25189 psig. Similarly, CF4 must decrease from 21.75566 to 14.50377 psig. Thus a total pressure of 7.25189/ 0.75= 9.66919 psig must be bled from the chamber. Finally, a 9.66919 psig of SF_6 must be administered to bring the total pressure up to ≈29.00 psig; the resulting mixture will then be 50% SF_6- 50% CF_4 mixture at 200 kPa. Mathematically, the mixing procedure is as follows:

29.00755= 7.25189	+	21.75566	(25% SF_6- 75% CF_4)
-2.41730		-7.25189	(bleeding off)
4.83459		14.50377	
+9.66918		0.00000	(filling with SF_6)
14.50377		14.50377	(50% SF_6- 50% CF_4)

Appendix B

Statistical Evaluation Of Test Results

From: IEC 60-2: 1973

Published by: British Standard Institution

A.1 Statement of the problem

As disruptive discharges are random phenomena, statistical procedures are useful to obtain more meaningful information from the measurements. It may be supposed that, for each test voltage U, there is a specific probability p of disruptive discharge occurring on any particular application. Some tests are aimed at a determination of the probability distribution function $p(U)$ relating p to the voltage U.

Usually, the probability distribution function is expressed in terms of the mean value U_M and the standard deviation σ of the disruptive discharge voltage. These parameters and the form of the function can be determined from tests made with a large number of voltage applications, provided that successive voltage applications do not significantly change the characteristics of the test object or, alternatively, if a fresh test object is used for each application.

Sometimes, for instance in certain impulse tests on external insulation, the probability distribution function is approximately Gaussian from some few percent up to 95% or even 98% disruptive discharge probability. Little information is available however on the character of the probability distribution function for internal insulation, with any type of voltage, and for external insulation, with direct and alternating voltages. Standard deviations are generally between 2% and 8%, but much larger values have been found during impulse tests on internal insulation.

Because in practical tests only a limited number of voltage applications can be made, the true values of U_M and σ can be estimated only within certain limits of accuracy, which (for a given degree of certainty) can be calculated (clause A.3). The measured values are designated $\bar{U}$ and s.

In the following, a brief summary is presented of some simple methods which are useful for the analysis of high voltage test results on test objects which are not affected by repeated applications (self-restoring insulation).

Note.- Attention is drawn to the fact that the probability distribution function is not necessarily symmetrical about the mean value. Hence, it is necessary to distinguish between the terms "mean value" and "most probable value".

A.2 Classification of tests

Disruptive discharge tests can be subdivided into three different categories for the purpose of statistical evaluation.

Class 1

Class 1 comprises tests made by repeated application of voltages of substantially constant shape in which, for each voltage level, the proportion of voltage applications causing disruptive discharge is recorded. It mainly applies to impulse tests, but certain alternating and direct voltage tests also fall into this class.

Class 2

Class 2 comprises procedures in which each application of the test voltage causes a disruptive discharge. The tests are made by applying continuously increasing voltages to the test object and by measuring the actual disruptive discharge voltages obtained. Such tests can be made with direct, alternating or impulse voltages. In particular, tests causing disruptive discharge on the front of the impulse fall into this class.

Class 3

Class 3 comprises tests made by repeated application of voltages of substantially constant shape in which the level, for each voltage applied, is determined by the result of the preceding voltage application, the first voltage applied being roughly equal to the estimated 50% disruptive discharge value.

A.2.1 *Analysis of results from class 1 tests*

The results of class 1 tests can be plotted on Gaussian linear paper (probability paper) with the voltage on the linear axis. If they lie approximately on a straight line, the distribution is approximately Gaussian. The voltage corresponding to a disruptive discharge probability p=0.5 can be used as an approximate determination of the mean value $\overline{U}$, and the voltage range between p=0.5 and p=0.16 as an estimate of s.

Other more accurate methods for determining $\overline{U}$ and s are found in the literature.

A.2.2 *Analysis of results from class 2 tests*

The results of class 2 tests appear as a series of n voltage values U_v from which estimates of the mean disruptive discharge voltage $\overline{U}$ and of the standard deviation s can be obtained:

$$\overline{U} = \frac{1}{n}\sum_{1}^{n} U_v$$

$$s = \sqrt{\left[\frac{1}{n-1}\sum_{1}^{n}(U_v - \overline{U})^2\right]}$$

Alternatively, the ratio $n_v/(n+1)$ can be plotted on probability paper as a function of U_v where n_v is the number of disruptive discharges up to and including the voltage U_v and n is the total number of voltage applications.

the curve permits a determination of $\overline{U}$ and s in the same manner as in Sub-clause A.2.1 but does not necessarily give the same results as the numerical method above.

A.2.3 *Analysis of results from class 3 tests*

A test procedure for making Class 3 tests and the method of analysis of test results so obtained to determine the 50% disruptive discharge voltage are described in Sub-clause 11.2.2 (Appendix B). For other methods and applications reference should be made to the literature.

A.3 Confidence limits

From any set of n measurements, statistical checks may be made to define limits between which the true mean value U_M and the true standard deviation σ may be stated to lie with a given probability p_c of this being correct. These limits are commonly expressed for p_c=0.95 and are then termed "95% confidence limits".

For Class 2 test results, and on the assumption that these have an approximately Gaussian distribution, the limits are given by the confidence limits for an arithmetic mean value. These are:

$$\overline{U} - st_p / \sqrt{n} \le U_M \le \overline{U} + st_p / \sqrt{n}$$

$$s\sqrt{(n-1) / \chi^2_{p/2}} \le \sigma \le s\sqrt{(n-1) / \chi^2_{(1-p/2)}}$$

where t_p, $\chi^2_{p/2}$, and $\chi^2_{(1-p/2)}$ are variable in the student's (t_p) and in the chi-square (χ^2) distribution for n-1 degrees of freedom with p=1-p_c. If no standard statistical table is available, the following table may be used for p_c=0.95.

n	$t_p / \sqrt{n}$	$\sqrt{(n-1)/\chi^2_{p/2}}$ (Lower limit)	$\sqrt{(n-1)/\chi^2_{(1-p/2)}}$ (Upper limit)
5	1.24	0.60	2.87
10	0.72	0.69	1.83
15	0.55	0.73	1.58
20	0.47	0.76	1.46
30	0.37	0.80	1.34
40	0.32	0.82	1.28
50	0.28	0.84	1.25

Note that the confidence limits of σ are symmetrical.

For n=20, the 95% confidence limits thus are given by:

$$\overline{U} - 0.47s \leq U_M \leq \overline{U} + 0.47s$$
$$0.76s \leq \sigma \leq 1.46s$$

In the case of Class 1 or Class 3 tests, other methods for the calculation of the confidence limits must be used, for which reference should be made to the literature.

A.4 Determination of voltage corresponding to very low or very high disruptive discharge probabilities

For some purposes, a determination is desired of voltage levels corresponding to very low or very high probabilities of disruptive discharge of the test object.

Conventional rated withstand tests or assured disruptive discharge tests such as described in Sub-clause 11.1 and 11.3 (IEC 60-2: 1973 "High-voltage testing techniques" Part 2. Test procedures) are neither intended, nor suitable for providing such information. The fact that a test object has passed such test procedures in itself gives little information concerning actual disruptive discharge probability.

Analysis of Class 1 test results as described in Sub-clause A.2.1 gives more information on the probability distribution, but this is still not adequate for determining the test voltage levels giving defined low or high disruptive discharge probabilities. A modified test procedure is therefore described below for determining the voltage level corresponding to a very low disruptive discharge probability. (For high probability, see note below.)

As a preliminary test, several sets of three voltage applications are made, starting at a level U_0 below the estimated withstand voltage. After every set, the voltage level is increased by a constant amount ε of between 2% and 5% of U_0. The series of tests are finished at the level U_1 when the first disruptive discharge occurs.

The test procedures are then continued in a similar manner, but with 25 voltage applications at each voltage level and starting at the level $U_2=U_1-3\varepsilon$. If no disruptive

discharge occurs, the voltage level is increased after each series of 25 by successive steps of the same amount ε, until a disruptive discharge occurs. When a disruptive discharge does occur, say during the series of applications at level U_2, the voltage then reduced in successive steps equal to 2ε until a full series of 25 applications has been applied with no disruptive discharge. Thereafter, the level is increased in steps equal to ε until one more disruptive discharge is obtained.

The test result is then taken as the highest voltage value which has not given disruptive discharge during any series of 25 voltage applications. This value corresponds to a disruptive discharge probability of about 1% and there is about 98% certainty that it will be less than 8%. Usually, the complete test requires about 75 voltage applications.

Note.- Almost identical procedures are used to determine the voltage corresponding to very high probabilities:

the foregoing description applies if the words "withstand" and "probability of withstand" are replaced by "disruptive discharge" and "probability of disruptive discharge". The voltage is first decreased from a high value instead of being increased from a low value.

A.5 **Conventional rated withstand and assured disruptive discharge tests**

The probability P of passing a conventional rated withstand test, as specified in Sub-clauses 11.1.2a and 11.1.3 (IEC 60-2: 1973 "High-voltage testing techniques" Part 2. Test procedures), is given by the polynomial distribution:

$$P = (1-p)^{15} + 15p(1-p)^{14} + \frac{15 \cdot 14}{2} p^2 (1-p)^{13}$$

where p is the probability of a disruptive discharge application at the test voltage.

Using the test procedures there described, therefore, and for a test voltage corresponding to p=0.10, the test object will have 0.82 probability P of passing the test. With p=0.01, the corresponding value is P=0.9995.

Similarly, an assured disruptive discharge voltage test, according to Sub-clause 11.3 (IEC 60-2: 1973 "High-voltage testing techniques" Part 2. Test procedures), gives the probability Q of passing the test, where:

$$Q = p^5 + 5(1-p)p^{14}$$

With p=0.9, the object will have 0.70 probability of passing the test and with p=0.99, the corresponding value is Q=0.994.